



HAL
open science

The dual-gate model for pentameric ligand-gated ion channels activation and desensitization

Marc Gielen, Pierre-Jean Corringer

► **To cite this version:**

Marc Gielen, Pierre-Jean Corringer. The dual-gate model for pentameric ligand-gated ion channels activation and desensitization. The Journal of Physiology, 2018, 10.1113/JP275100 . pasteur-01721186

HAL Id: pasteur-01721186

<https://pasteur.hal.science/pasteur-01721186>

Submitted on 6 Mar 2018

HAL is a multi-disciplinary open access archive for the deposit and dissemination of scientific research documents, whether they are published or not. The documents may come from teaching and research institutions in France or abroad, or from public or private research centers.

L'archive ouverte pluridisciplinaire **HAL**, est destinée au dépôt et à la diffusion de documents scientifiques de niveau recherche, publiés ou non, émanant des établissements d'enseignement et de recherche français ou étrangers, des laboratoires publics ou privés.



Distributed under a Creative Commons Attribution - NonCommercial 4.0 International License

The dual-gate model for pentameric ligand-gated ion channels activation and desensitization

Marc Gielen* & Pierre-Jean Corringer

Channel Receptors Unit, CNRS UMR 3571, Institut Pasteur, Paris, France

Abstract

Pentameric ligand-gated ion channels (pLGICs) mediate fast neurotransmission in the nervous system. Their dysfunction is associated with psychiatric, neurological and neurodegenerative disorders such as schizophrenia, epilepsy and Alzheimer's disease. Understanding their biophysical and pharmacological properties, both at the functional and structural levels, thus holds many therapeutic promises. In addition to their agonist-elicited activation, most pLGICs display another key allosteric property, namely desensitization, in which they enter a shut state refractory to activation upon sustained agonist binding. While the activation mechanisms of several pLGICs have been revealed at near-atomic resolution, the structural foundation of desensitization has long remained elusive. Recent structural and functional data now suggest that the activation and desensitization gates are distinct, and are located at both sides of the ion channel. Such a "dual gate mechanism" accounts for the marked allosteric effects of channel blockers, a feature illustrated herein by theoretical kinetics simulations. Comparison with other classes of ligand- and voltage-gated ion channels show that this dual gate mechanism emerges as a common theme for the desensitization and inactivation properties of structurally unrelated ion channels.

Abbreviations: 5HT₃R, 5HT₃ serotonin receptor; DAM, desensitization-modifying allosteric modulator; DHA, docosahexaenoic acid; EC₅₀, half maximal effective concentration; ECD, extracellular domain; ELIC, *Erwinia* ligand-gated ion channel; GABA, γ -Aminobutyric acid; GABA_AR, GABA_A receptor; GlyR, glycine receptor; GLIC, *Gloeobacter* ligand-gated ion channel; IC₅₀, half maximal inhibitory concentration; iGluR, ionotropic glutamate receptor; MWC, Monod-Wyman-Changeux; nAChR, nicotinic acetylcholine receptors; NAM, negative allosteric modulator; PAM, positive allosteric modulator; pLGIC, pentameric ligand-gated ion channel; PS, pregnenolone sulfate; SAM, silent allosteric modulator; TEVC, two-electrode voltage clamp; TMD, transmembrane domain

Acknowledgements

The authors would like to thank Jean-Pierre Changeux for critical reading of the manuscript.

This is the accepted version of the following article: Gielen, M. and Corringer, P.-J. (), The dual-gate model for pentameric ligand-gated ion channels activation and desensitization. J Physiol. Accepted Author Manuscript. doi:10.1113/JP275100, which has been published in final form at <https://doi.org/10.1113/JP275100>. This article may be used for non-commercial purposes in accordance with Wiley Terms and Conditions for Self-Archiving.

*Corresponding author: M. Gielen, marc.gielen@pasteur.fr

1. Introduction

Ionotropic receptors are responsible for fast chemical neurotransmission. Upon binding of their agonist, the transmembrane pore of these receptors quickly opens to enable the selective flow of permeant ions across the plasma membrane. Amongst ionotropic receptors, the superfamily of pentameric ligand-gated ion channels (pLGICs) comprises excitatory serotonin receptors and nicotinic acetylcholine (nAChRs), the latter contributing notably to higher brain functions such as cognition and reward (Changeux, 1990), as well as chloride-permeable γ -Aminobutyric acid (GABA) type A receptors (GABA_ARs) and Glycine receptors (GlyRs), which mediate fast inhibitory synaptic transmission in the central nervous system of vertebrates. This superfamily was formerly known as the Cys-loop family, since all animal pLGICs contain a conserved disulphide bridge. However, following the discovery of bacterial homologs devoid of the corresponding cysteines (Tasneem et al., 2005; Bocquet et al., 2007), these receptors were regrouped under the generic name of pLGICs. More recently, the name of “Pro-loop receptors” has been proposed based on the presence of a strictly conserved proline in the “Cys-loop” region (Jaiteh et al., 2016). In line with their paramount physiological importance, pLGICs are primary targets for pharmacological treatments of a wide range of diseases: benzodiazepines, which positively modulate GABA_ARs, are used to treat anxiety and epilepsy (Galanopoulou, 2008; Nuss, 2015), while drugs targeting nAChRs are investigated as potential cure for various diseases including Alzheimer’s disease, schizophrenia and tobacco addiction (Taly et al., 2009).

A wealth of structural studies has recently improved our understanding as to how pLGICs activate at the near-atomic level. Indeed, the structures of two prokaryotic pLGICs were solved by X-ray crystallography almost a decade ago: the *Erwinia* ligand-gated ion channel ELIC (Hilf and Dutzler, 2008), which is activated by a series of amino acids including GABA, and the proton-activated *Gloeobacter* ligand-gated ion channel GLIC (Bocquet et al., 2007, 2009). Several X-ray structures of eukaryotic pLGICs followed in the past years: the *C. elegans* glutamate-gated chloride channel (GluCl) (Hibbs and Gouaux, 2011), the mouse 5HT_{3A}R (Hassaine et al., 2014), the human β 3 GABA_AR (Miller and Aricescu, 2014) and the human α 3 GlyR (Huang et al., 2015), the zebrafish α 1 GlyR being the first member of the family to be examined by single-particle cryo-electron microscopy (cryo-EM; Du et al., 2015), and finally the α 4 β 2 nAChR (Morales-Perez et al., 2016), i.e. the first structure of a heteromeric pLGIC since the medium-resolution cryo-EM structure of the Torpedo muscle-type nAChR (Miyazawa et al., 2003).

All these data show an overall conservation of pLGICs’ architecture, where all five subunits arrange in a ring-like structure, with a pseudo five-fold axis of symmetry coinciding with the ion channel (Fig. 1A; Cecchini and Changeux, 2015). This stereotypical architecture includes the location of the orthosteric site where the transmitter binds: it is located at the N-terminal extracellular domain (ECD), at the interface between adjacent subunits. The ECD of each subunit, formed by a β sandwich, is connected to the transmembrane domain (TMD), composed of four membrane-spanning α -helical segments, named M1-M4. The M2 segments line the pore, allowing the selective flow of permeant ions in the open conformation of the channel (Giraudat et al., 1986; Imoto et al., 1988; Leonard et al., 1988). Amidst this well-ordered modular architecture, the M3-M4 loop is involved in the trafficking of the receptors

to the plasma membrane, their anchoring at the synapse, and their modulation by intracellular interactions and phosphorylation (Smart and Paoletti, 2012; Langlhofer and Villmann, 2016). While the central portion of this cytoplasmic loop is a highly variable and flexible region, the post-M3 and pre-M4 regions fold into α -helices called MX and MA, respectively (Hassaine et al., 2014). The latter is involved, in particular, in the ionic conductance of the channel (see below).

2. Gating mechanism and permeation determinants of pLGICs

During fast synaptic transmission, vesicular fusion leads to the brief release of a high concentration of neurotransmitters (typically 1 mM), which remain in the synaptic cleft for a duration of ~ 1 ms (Katz and Miledi, 1973; Kuffler and Yoshikami, 1975; Attwell and Gibb, 2005). Most neurotransmitter-gated channels, and synaptic pLGICs in particular, have been selected by evolution for their fast activation and deactivation kinetics, which allows them to stay tuned for activation after a minimal time lapse and to follow high frequency vesicular fusions evoked by trains of action potentials (Papke et al., 2011). Fast deactivation kinetics notably involves a high dissociation rate for the agonist, which translates into a low apparent affinity for the agonist. On the contrary, extra-synaptic types of pLGICs may display a higher apparent affinity for the agonist, as generally seen for GABA_ARs (Mortensen et al., 2011), making them able to react to low concentrations of agonists encountered during volume transmission (Vizi et al., 2010; Trueta and De-Miguel, 2012).

Activation of pLGICs have long been analysed according to a minimal 2-states model, the receptor equilibrating between a resting (shut) state and an active (open) state. In particular, the Monod-Wyman-Changeux (MWC) model has been thoroughly used, whereby the receptor can readily visit both conformations in the absence of agonist, the latter simply shifting the conformational equilibrium towards the open state (Monod et al., 1965; Einav and Phillips, 2017). The strongest argument in favour of the MWC model resides in the spontaneous openings measured in the absence of agonist, initially described for mouse muscle-type nAChRs (Jackson, 1984). Such spontaneous activity gives rise to robust constitutive currents in cells expressing mutant pLGICs endowed with strong gain-of-function phenotypes (Purohit and Auerbach, 2009; Colquhoun and Lape, 2012). Still, in the past decade, single-channel studies, performed on GlyRs and nAChRs, identified intermediates between the resting and open states of the receptors, which we generically name here “pre-active” states. They carry a closed channel and are transiently stabilized by agonists. The pre-active state called “flipped” is partly stabilized by partial agonists, explaining why they elicit only a fraction of the response elicited by full agonists (Lape et al., 2008). The pre-active states called “primed” explain why low concentrations of agonist do elicit short-lived open states (through stabilization of a partially primed state), which are kinetically distinct from the long-lived ones occurring under higher concentrations (through stabilization of a fully primed state) (Mukhtasimova et al., 2009). More recently, a “catch and hold” mechanism has been proposed, stipulating that the binding of agonists promotes a first conformational change leaving the binding site in a low affinity state (“catch”), subsequently followed by another isomerization step resulting in a high affinity pre-active state (“hold”; Purohit et al., 2014;

Nayak and Auerbach, 2017). This scheme explains the apparent paradox that structurally related agonists display markedly different association constants for the resting state. The “catch and hold” model may be seen as a refinement over the idea behind the priming model, which might correspond to the “hold” step; and the priming model may itself be seen as a refined version of the flipping model, in which conformational changes at distinct subunits are considered individually (Plested, 2014). In parallel, rate-equilibrium free-energy relationships suggest that pLGICs’ activation pathway contains multiple brief intermediates (Grosman et al., 2000), possibly indicating an even larger repertoire of pre-active states accessible to the nAChRs. The concept of pre-active states was further extended to GABA_ARs, since the positive allosteric modulators (PAM) benzodiazepines were shown to facilitate a pre-activation step at GABA_ARs (Gielen et al., 2012; Dixon et al., 2015), similarly to the action of the allosteric modulator NS-9283 at $\alpha 4\beta 2$ nAChRs (Indurthi et al., 2016).

Interestingly, three pLGICs, GLIC, GluCl and the zebrafish $\alpha 1$ GlyR, have been solved in several conformations, highlighting some key allosteric reorganization associated with channel opening (Prevost et al., 2012; Sauguet et al., 2014; Althoff et al., 2014; Du et al., 2015). Comparison of the structures solved in the absence and presence of agonist suggests a common mechanism of activation whereby agonists stabilize the ECD in a contracted (“unbloomed”) conformation, and the entire receptor in a twisted conformation (Nemecz et al., 2016). Importantly, normal mode analysis and molecular dynamics simulations are consistent with this bloom & twist activation mechanism (Taly et al., 2006; Calimet et al., 2013). As a cautionary note, the interpretation of MD trajectories relies on the assignment of functional states to the structures used as starting points for the simulations, and it has been proposed that the initial GLIC and GluCl structures might represent desensitized states (Akabas, 2013). Still, recent molecular dynamics suggests that the main quaternary event concomitant with channel opening lies in the twisting (Martin et al., 2017). This quaternary motion is coupled to a tilt of the M2 pore-lining helices, yielding a widening of the upper part of the channel that carries the activation gate. It consists in two or three rings of hydrophobic residues encompassing the 9’ and 13’ M2 residues that form an hydrophobic barrier to ion permeation, which is released upon channel opening (see Fig. 2 and Jaiteh et al., 2016 for numbering conventions). These structural features, including the binding sites for agonists and allosteric modulators, have been extensively described in recent review articles (Corringer et al., 2012; daCosta and Baenziger, 2013; Cecchini and Changeux, 2015; Nemecz et al., 2016), and will not be reviewed here in detail.

It is noteworthy that the structural reorganizations underlying the above-mentioned pre-active states remain unknown. However, recent work on the prokaryotic GLIC recently identified and characterized structurally such an intermediate. Indeed, using the tryptophan-induced fluorescence quenching method, Menny et al. managed to follow the structural dynamics of a fully functional GLIC protein reconstituted into liposomes (Menny et al., 2017). Data show that the agonist promotes a fast quaternary compaction of the ECD concerted with a key revolving motion of the M2-M3 loop at the ECD-TMD interface. This global pre-activation step is followed by a slower opening of the channel to elicit the electrophysiological response. Interestingly, similar protein motions are found in a particular X-ray conformation of GLIC, named the “locally-close-LC2” conformation, where the ECD has undergone the transition

toward the active state-like conformation, but where the TMD still remains in a resting state-like conformation (Fig. 1B; Prevost et al., 2012). The symmetrical nature of this ECD-compacted LC2 conformation might be representative of a flipped (or fully primed) state.

Once the channel gate is open, ions flow according to their electrochemical gradient and the selectivity and conductance of the channel. The major determinant of ionic selectivity, namely the selectivity filter, lies at the cytoplasmic end of the pore (Imoto et al., 1988; Leonard et al., 1988), at the M2 -1' level for most eukaryotic cationic pLGICs and at the M2 -2' level for anionic ones, the latter featuring an insertion in this region. Indeed, cation-permeable pLGICs harbour an acidic residue at the -1' position, providing a favourable electrostatic environment for the coordination of positively charged ions, and mutating this residue, together with a proline insertion at position -2', converts the cationic $\alpha 7$ nAChR into an anion-permeable channel (Corringer et al., 1999). Moreover, other important determinants in the vicinity of the -1'/-2' residue have been identified, such as the protonation of the buried 0' basic residue (Cymes and Grosman, 2011) or the side-chain orientation of neighbouring protonable residues (Cymes and Grosman, 2016). A 2.4 Å resolution structure of GLIC in its putative open conformation further revealed the organization of water pentagons, which coordinate permeant ions in the 2'/6' region (Sauguet et al., 2013). Besides the canonical selectivity filter, two other regions have been shown to participate in the conductance of pLGICs. First, the extracellular vestibule, which prolongs the transmembrane pore in the inner part of the ECD, can provide an electrostatic environment through which permeant ions flow and thus participate in the ionic conductance (Hansen et al., 2008), although this region doesn't appear to affect ionic selectivity (Cymes and Grosman, 2016). Second, charged residues in the intracellular domain, located in the MA segment upstream of the M4 N-terminus, line a putative lateral exit serving as an intracellular ionic portal (Hassaine et al., 2014). Their charge thus influences the passage of permeant ions, a mechanism that explains the differential conducting properties between 5HT_{3A} and 5HT_{3B} receptors (Kelley et al., 2003).

3. Desensitization of pLGICs: the case study of the muscle-type nAChR

Besides the agonist-elicited activation, most pLGICs display another fundamental property: desensitization. Indeed, for most pLGICs, the sustained presence of the neurotransmitter causes the channels to transit from the active agonist-bound conformation to an agonist-bound shut-channel one called the desensitized state, thereby decreasing current flow (Katz and Thesleff, 1957). Desensitization is thought to prevent the over-activation of receptors in pathological conditions, and can also lead to the reduction of postsynaptic current upon repetitive synaptic neurotransmitter release (Changeux, 1990; Jones and Westbrook, 1996; Papke et al., 2011). Functional studies, mostly performed on muscle-type nAChRs during the 1980s and the 1990s, highlighted a series of kinetic features of desensitization:

- 1) Desensitization kinetics are multiphasic: stopped-flow binding experiments, performed on nAChRs from *Torpedo marmorata* membranes, directly revealed the existence of distinct “fast” and “slow” desensitized states, and that 20% of unliganded nAChRs are in a desensitized high-affinity state in this preparation (Heidmann and Changeux, 1979, 1980; Boyd and Cohen, 1980). In parallel, electrophysiological recordings showed up to five

temporal components of desensitization in the milliseconds to minutes time-range (Feltz and Trautmann, 1982; Elenes and Auerbach, 2002; Papke et al., 2011). As a result, desensitization is classically portrayed as a two-components phenomenon stemming from the existence of distinct “fast” and “slow” desensitized states (Edelstein et al., 1996). Of note, the desensitization kinetics of pLGICs is often highly variable, complicating experimental investigation (see Box 1);

2) The macroscopic desensitization rate (i.e. the rate of temporal decline of ensemble macroscopic currents) increases linearly with the open probability of muscle-type murine nAChRs, suggesting that desensitization mainly proceeds from a fully liganded state (Dilger and Liu, 1992; Franke et al., 1993). Auerbach and Akk took this work further, and showed that desensitization of muscle-type mouse nAChRs occurs mostly from the diliganded active state (Auerbach and Akk, 1998);

3) Concerning the recovery from desensitization following agonist removal, the main pathway involves first agonist dissociation from the desensitized receptor, and then the unbound desensitized receptor undergoes a rate-limiting isomerization toward the resting state (Katz and Thesleff, 1957; Cachelin and Colquhoun, 1989; Dilger and Liu, 1992; Franke et al., 1993). This scheme is also largely applicable to GABA_ARs, for which functional recovery from desensitization is about four-fold slower than the dissociation of radiolabelled agonist (Chang et al., 2002). Still, this ratio enables some GABA_ARs receptors to recover from desensitization through the liganded open state, which in turn allows the receptors to open after sojourns in desensitized states and prolongs deactivation kinetics after desensitization (Jones and Westbrook, 1995). While initial models suggested a direct transition from an agonist-unbound desensitized state to an agonist-unbound resting state, further modelling indicated that a transition through the active state cannot be discarded, even in the absence of measurable openings of the channel (Edelstein et al., 1996). Indeed, the unliganded openings are so brief that most would escape electrophysiological detection.

4. Mutations affecting the desensitization properties of pLGICs

Seminal site-directed mutagenesis work revealed that mutations of the hydrophobic M2 9' residue, most commonly a leucine, into small polar threonine or serine residues, almost fully ablate desensitization of $\alpha 7$ nAChRs (Revah et al., 1991); analysis of homologous mutations extended this result to the entire pLGIC family (Yakel et al., 1993; Bianchi and Macdonald, 2001). Since then, many mutations have been found to affect macroscopic desensitization. Strikingly, such mutations are scattered throughout the entire sequence of the receptors (see Zhang et al., 2013 for review). At the level of the ECD, for instance, the W55A mutation ablates the desensitization of $\alpha 7$ nAChRs (Gay et al., 2008), while the ECD-TMD interface is a hotspot for mutations with pronounced loss-of-desensitization phenotypes, as illustrated by a series of $\alpha 7$ nAChRs mutants (Bouzat et al., 2008; Wang and Lynch, 2011; Zhang et al., 2011).

In recent years, though, various studies pointed out an involvement of the cytoplasmic end of the pore in the desensitization of GlyRs. Analysis of patients with hyperekplexia has led to the

investigation of mutations nearby the selectivity filter (M1-M2 loop) of the GlyR $\alpha 1$, such as the GlyR $\alpha 1^{I244A}$ and $\alpha 1^{P250T}$, which produce a loss-of-function phenotype accompanied by strong increases in the desensitization kinetics (Fig. 2; Lynch et al., 1997; Saul et al., 1999; Breitingner et al., 2004). Further work showed the involvement of intracellular M3-M4 linker mutation or splice variant in desensitization (Papke and Grosman, 2014; Langlhofer and Villmann, 2016).

Recently, we constructed a series of chimeras between the $\alpha 1\beta 2$ heteromeric and $\rho 1$ homomeric GABA_ARs, which show contrasted desensitization properties (Gielen et al., 2015). It revealed that interactions between the M1-M2 linker and the intracellular end of M3 of an adjacent subunit shape macroscopic desensitization. In the course of our mutagenesis work, we then focused on the intracellular end of the M2/M3 interface, and found a series of residues whose mutation drastically increases desensitization, rendering it almost total and increasing its on-rate kinetics by up to hundred-fold (Fig. 2; Gielen et al., 2015). We obtained similar results for GlyRs, indicating a conserved mechanism for anionic pLGICs.

It is noteworthy that, since desensitization mainly occurs downstream of the receptor's activation (Auerbach and Akk, 1998), a mutation specifically affecting the receptor's microscopic activation kinetics could profoundly impact the macroscopic desensitization kinetics. Hence, for most of the above-mentioned mutations, which also strongly alter the activation of pLGICs, the effect on desensitization remains ambiguous. However, the single-site mutations at the intracellular end of the M2/M3 of GABA_ARs minimally affect their GABA and benzodiazepine dose-response curves (Gielen et al., 2015), supporting that they selectively affect desensitization.

5. A desensitization gate at the intracellular end of the pore, distinct from the activation gate

Given the location of those M2/M3 interface mutations, we hypothesized that desensitization might involve the closure of the pore at its intracellular end. To test that hypothesis, we used the pore blocker picrotoxin, which binds in this M2 -2' / 2' region (Fig. 3A; Hibbs and Gouaux, 2011).

We suspected that picrotoxin could prevent desensitization by a foot-in-the-door mechanism, i.e. by physically hindering the constriction of the channel, and thus investigated a potential inhibition of desensitization by picrotoxin binding (Fig. 3B). Such mechanism is clearly apparent for the $\alpha 1$ GlyR: following prolonged co-application of saturating concentrations of the agonist glycine and picrotoxin, wash-out of picrotoxin reveals a prominent rebound current (Fig. 3C). This rebound current is perfectly reproduced in a kinetic scheme, in which picrotoxin binding fully prevents desensitization (Gielen et al., 2015).

These results demonstrate that the activation and desensitization gates are distinct, at least for the slow-desensitization component that is investigated here. A similar idea was speculated early on by Auerbach and Akk from single-channel recordings of muscle-type nAChRs, assessing primarily fast desensitization components (Auerbach and Akk, 1998; Purohit and Grosman, 2006). Altogether, our results are consistent with picrotoxin preventing

desensitization by a foot-in-the-door mechanism, the lower part of the channel fulfilling two functions: the selectivity filter and the desensitization gate.

6. The detailed analysis of picrotoxin block of anionic pLGICs requires the inclusion of an effect on activation

In addition to the rebound current described above, picrotoxin binding results in a loss of apparent affinity for the agonist by approximately one to two orders of magnitude, i.e. a so-called “competitive” rightward shift in the dose-response curve for the agonist at both GABA_ARs (Smart and Constanti, 1986; Goutman and Calvo, 2004; Qian, 2004) and GlyRs (Lynch et al., 1995; Wang et al., 2006, 2007). At sub-activating agonist concentrations, picrotoxin also promotes agonist dissociation by stabilizing the resting conformation, as shown by voltage-clamp fluorometry of GABA_ARs (Chang and Weiss, 2002). It could thus be argued that the rebound current observed upon picrotoxin wash-out could actually reflect the stabilization of the resting state over the active state, similarly to competitive antagonists (Xu et al., 2016), rather than preventing desensitization.

To investigate these possibilities, we built simplified kinetic models of picrotoxin block of GlyRs containing a minimal number of steps: 1) agonist binding, 2) channel opening, 3) desensitization and 4) picrotoxin binding. Figure 3 shows illustrating traces assuming that picrotoxin stabilizes the resting channel, i.e. that picrotoxin decreases the microscopic opening rate by a factor ρ . In a first model, picrotoxin binding prevents the desensitization of $\alpha 1$ GlyRs (Fig. 3D), while it can bind and be trapped in desensitized receptors in the second model (Fig. 3E). The first model results in non-distinguishable rebound currents for the values $\rho=1$ and $\rho=10$. However, the rebound current is strongly decreased in the case in which $\rho=100$ (Fig. 3F). Indeed, in this situation and with our set of kinetic values, picrotoxin largely stabilizes the resting shut state of the channel (i.e. the opening rate β becomes smaller than the shutting rate α), but cannot dissociate from it. Picrotoxin thus presents an “auto-trapping” phenomenon at high ρ values, which slows down its apparent dissociation rate and limits the amount of rebound current. Of note, a ten-fold decrease in gating efficacy of human $\alpha 1$ GlyRs upon picrotoxin binding is consistent with previous studies (Wang et al., 2006). On the other hand, no set of parameter with the second model can reproduce a prominent rebound current with ρ values in the 1-100 range (Fig. 3G), further arguing that picrotoxin indeed prevents the desensitization of inhibitory pLGICs. Moreover, if the channel adopted an identical conformation in the resting and desensitized states, picrotoxin should actually stabilize the desensitized state over the open one in that second model (i.e. picrotoxin binding should decrease d' in Fig. 3E). Such mechanism should lead to an increased desensitization in our protocol, resulting in a large slow component of current recovery after picrotoxin wash-out, unlike what is observed experimentally.

The pore-block mechanism by picrotoxin, which not only prevents desensitization but also stabilizes the channel in a resting state, probably accounts for the complex interplay between picrotoxinin (i.e. the most active part of picrotoxin, which is an equimolar mixture of picrotoxinin and picrotin) and the allosteric potentiator ivermectin at zebrafish $\alpha 1$ GlyRs. The structure of this receptor has been solved in three different conformations by cryo-EM: apo,

glycine-bound and glycine- plus ivermectin-bound, the latter proposed to represent either a desensitized or a partially open state (Du et al., 2015). In the presence of ivermectin, the zebrafish $\alpha 1$ GlyR was shown to desensitize on a timescale of several minutes. Interestingly, in the presence of an approximate EC_{50} concentration of glycine, 1 mM picrotoxinin inhibits the zebrafish $\alpha 1$ GlyR by $\sim 80\%$, but inhibition drops to $\sim 20\%$ in the presence of ivermectin (Du et al., 2015). It is likely that ivermectin simply reduces the apparent affinity for picrotoxinin by decreasing the likelihood for the channel to visit its picrotoxinin high-affinity state, namely its resting state, without any effect of ivermectin on desensitization. This hypothesis is illustrated in the kinetic model from Figure 4A-B, leading to simulations that account well for experimental observations (Fig. 4C).

Such kinetic model, in which ivermectin does not affect the microscopic desensitization step, predicts that ivermectin will not increase desensitization under high glycine concentrations (Fig. 4D). In that hypothesis, it is unclear why the zebrafish $\alpha 1$ GlyR adopts two different conformations under glycine alone or glycine plus ivermectin conditions (Du et al., 2015). Importantly, recent structural and modelling work suggests that the bona fide open structure of pLGICs most likely resembles the open structures of GLIC and GluCl, rather than the much larger pore conformation of the cryo-EM structure of the zebrafish $\alpha 1$ GlyR bound to glycine alone (Gonzalez-Gutierrez et al., 2017). A contrario, recent MD simulations suggest that the wide open zebrafish $\alpha 1$ GlyR structure is conductive, while the ivermectin- and glycine-bound $\alpha 1$ GlyR structure should not conduct ions (Trick et al., 2016). In these simulations, however, it is unclear whether the simulated conduction properties of the wide-open zebrafish $\alpha 1$ GlyR match the experimentally derived values, nor is it possible to infer how much structural change is required to convert the ivermectin- and glycine-bound $\alpha 1$ GlyR structure into a conductive conformation. Further work will thus be required to assign a functional annotation to the zebrafish $\alpha 1$ GlyR conformations.

7. Structural data corroborate the desensitization gate model

In agreement with the above-mentioned functional work, recent X-ray studies provide a structural counterpart to the analysis of the desensitization gate. Miller and Aricescu published in 2014 the structure of the homomeric $\beta 3$ GABA_AR in complex with its agonist benzamidine (Miller and Aricescu, 2014). This structure shows a wide open activation gate in the M2 9'/13' region, but a hydrophobic constriction at the -2' proline, where the pore radius narrows down to 1.6 Å, thereby precluding the flow of chloride ions whose Pauling radius is 1.8 Å. More recently, several pLGICs have been solved in similar conformations: the human $\alpha 3$ GlyR in complex with both glycine and a positive allosteric modulator, AM-3607 (Huang et al., 2017), as well as a GLIC-(GABA_A $\alpha 1$) and a (GABA_A $\beta 3$)-(GABA_A $\alpha 5$) chimera, the former carrying a $\alpha 1^{G258V}$ mutation promoting desensitization (Lavery et al., 2017; Miller et al., 2017). All these structures show a conserved pore conformation and were assigned to a desensitized state, since they correspond to agonist-bound shut states. In addition, they account for the above functional work that identified the desensitization gate nearby the binding site for picrotoxin, which comprises the -2' residue.

Comparing these structures to the putative open GLIC and GluCl suggest that, during the transition from the active to the desensitized state, a symmetrical tilt and rotation of the M2 helices narrows down the cytoplasmic constriction while widening the upper part of the channel (Fig. 5A). At the level of the 9' residue, this latter “pull & twist” motion generates a rotation of the side-chain away from the lumen of the pore to point towards a neighbouring M2 segment (Fig. 5A). This local motion probably contributes to the marked “gain of function” phenotype observed when the 9' residue is mutated to more hydrophilic residue. Indeed, such mutations are expected to stabilize preferentially the active conformation with a 9' side chain facing the polar aqueous environment, consistent with functional studies (Bianchi and Macdonald, 2001).

Does this mechanism of desensitization also pertain to cationic pLGICs such as nAChRs? The $\alpha 4\beta 2$ nAChR structure may illustrate this proposal (Morales-Perez et al., 2016): the M2 α -helices are well superimposable when comparing the $\alpha 4\beta 2$ nAChR structure to the structures of anionic pLGICs in putative desensitized conformations (Fig. 5B), including the orientation of the M2 9' residue. This is consistent with the $\alpha 4\beta 2$ nAChR structure being representative of a desensitized state. The M2 -1' nAChR glutamate residues, the major contributor to the selectivity filter, form the most constricted part of the channel, leading to a pore diameter akin to the ones observed for putative desensitized structures of anionic pLGICs (Miller et al., 2017). However, the relationship between pore diameter and conduction property is complicated by two issues in this case: first, the constriction at -1' is hydrophilic and even negatively charged, and it is unclear by which mechanism such a pore, which would provide a microenvironment favourable for cations, would impair their permeation. Second, the M2 -1' glutamates are fixed in a symmetrical conformation in the crystal structure, whereas the residue side-chains are dynamic and certainly adopt a variety of rotameric conformations in solution, potentially widening the effective pore diameter (Rossokhin and Zhorov, 2016). Such point is all the more important since the rotameric conformations of the M2 -1' glutamates have been proposed to control the conductance of nAChRs (Harpole and Grosman, 2014). Further work is thus required to fully understand the exact determinants for nAChRs desensitization.

Thus, similar desensitization mechanisms might indeed be conserved amongst both anionic and cationic pLGICs, with the existence of distinct activation and desensitization gates. Consistent with this idea, diverse pore-blockers have been shown to differentially stabilize the resting, active and desensitized states of both anionic pLGICs and muscle-type nAChRs (see Box 2). The desensitization gate model may thus be extended to the entire pLGIC family, where the full gating cycle would include: 1) a pre-activation step involving the ECD “unblooming”; 2) channel activation gate opening, in the upper half of the pore, concomitant with the ECD-TMD interface rearrangement and the whole receptor “twisting”; 3) channel desensitization resulting from the constriction of the desensitization gate at the intracellular end of the pore (Fig. 6).

8. Reconciling the DHA-bound structure of GLIC with a dual gate model

Recently, an X-ray structure of the bacterial pLGIC GLIC in complex with the fatty acid docosahexaenoic acid (DHA) revealed a new pore conformation, with a profile intermediate between that of the putative resting and open states of the channel (Basak et al., 2017): the activation gate has transitioned towards the open channel conformation, with the exception of the M2 9' residue that still shapes a hydrophobic constriction in the middle of the pore.

To propose a functional annotation of this apparently shut state, Basak et al. performed a series of electrophysiological experiments showing that: 1) The co-application of DHA with an activating acidic solution produces no alteration of the fast time response to protons, but a slow and progressive inhibition as if DHA favoured a desensitization process, 2) DHA produces a slight decrease in the EC_{50} of activation by protons and 3) DHA fails at inhibiting the proton-elicited currents of the I9'A mutant of GLIC.

Based on these data, it was proposed that DHA stabilizes the desensitized state of GLIC, which would account for the decrease in the proton EC_{50} and the I9'A mutant phenotype, since this mutation is believed to prevent desensitization. However, the X-ray structure of the GLIC-DHA complex looks more like an intermediate state in the activation pathway than a desensitized state as discussed above. We thus investigate an alternative possibility herein that DHA may stabilize an intermediate pre-active state.

Figure 7 shows a purely theoretical kinetic scheme of a receptor, in which the resting state binds an agonist, then enters a pre-active state and can subsequently activate. In this scheme, binding of an allosteric inhibitor that selectively stabilizes the pre-active state (Fig. 7A&B) produces both an increase in the pre-activation constant, and a decrease in the activation constant (Fig. 7C). It will drive the receptor away from the active state to lower the open probability (Fig. 7D), but also promotes the overall population of agonist-bound state to increase the apparent affinity for the agonist (i.e. it decreases the agonist EC_{50}) (Fig. 7D). Therefore, an allosteric inhibitor increasing the apparent affinity for the agonist can do so by either promoting a pre-active or a desensitized state.

As an illustration, Figure 8 provides a kinetic model of GLIC (Fig. 8A&B), which expands the one presented in Figure 7 by adding a desensitization step from the active state. This kinetic model reproduces all aspects of GLIC activation by protons and its inhibition by DHA. First, DHA co-application produces an increase in the rate and the extent of current loss upon prolonged proton applications (Fig. 8C). Second, the concentration-response curve for DHA yields an IC_{50} value broadly consistent with the inhibition measured experimentally (Fig. 8D). Finally, and most importantly, DHA increases the apparent affinity of GLIC for protons when measured either at peak or steady state currents (Fig. 8E&F).

Another argument for DHA stabilizing a desensitized state is the inability of DHA to inhibit GLIC 9' mutants. However, M2 9' mutations not only ablate desensitization, they actually stabilize the open state of the pore over both resting and desensitized shut states (Bianchi and Macdonald, 2001). In Figure 9 is depicted a kinetic model of GLIC functioning, whereby the M2 9' mutation selectively stabilizes the open state over all the other states (Fig. 9A&B). Two schemes are then considered: in scheme I, the inhibitor DHA selectively stabilizes the desensitized state; whereas in scheme II, the inhibitor DHA selectively stabilizes the pre-active state (Fig.9C). In both schemes, the effects of DHA and the M2 9' mutation are

considered additive. Using the set of parameters from Figure 8, the 9' mutation is predicted to fully prevent DHA inhibition in both schemes (Fig. 9D).

As a conclusion, the whole set of experiments are equally accounted assuming either a stabilization of the desensitized (scheme I) or the pre-active state (scheme II) by DHA. However, the two schemes make quite different predictions regarding the short-term effect of DHA on the proton-elicited response, since in scheme II DHA should strongly affect the peak response, while in scheme I DHA should only affect the downstream process of desensitization. As illustrated with the kinetic models shown in Figures 8 and 9, if we equilibrate GLIC with DHA at neutral pH, and then apply acidic pH in the continued presence of DHA, we observe no inhibition (versus robust inhibition) of the peak proton-elicited current in scheme I (versus scheme II) (Fig. 10A,B). Incidentally, such experiment has been made, and DHA pre-application is indeed shown to elicit robust inhibition of the GLIC peak response elicited by protons (Basak et al., 2017), consistent with DHA affecting a pre-activation step. Moreover, with simple linear schemes as the ones presented here, and if we assume that desensitization kinetics remain slower than activation kinetics, the agonist concentration-response curve for *peak* responses should not be affected by a drug modulating desensitization. The DHA-induced increase in apparent affinity for protons, as measured with peak responses (Basak et al., 2017), is thus another argument in favour of DHA modulating the pre-activation step (Fig. 8F).

Of course, it is still possible that more complex kinetic models, in which direct resting-to-desensitized transitions are possible in the absence of agonist for example, could account for these experimental results. However, the presently developed simple kinetic models provide arguments that the DHA-bound structure of GLIC actually represents that of a pre-active state. Interestingly, electron paramagnetic resonance measurements suggest that the M4 segments undergo an outward movement during desensitization, and double electron-electron resonance experiments indicate that the distance between M4 segments increases during desensitization (Basak et al., 2017). These results do not agree with the DHA-bound structure representing a desensitized state, since the M4 segments are superimposable in the DHA-bound and in the putative open and resting states of GLIC (Basak et al., 2017). Thus, the DHA-bound structure may well represent an intermediate pre-active shut state, and this interesting one-of-a-kind structure could help in delineating the activation transition pathway of pLGICs. However, a definitive answer to the pre-activation versus desensitization hypotheses of DHA modulation might only be provided by single-channel recordings: an effect on desensitization should decrease the mean cluster duration, while an effect on pre-activation should decrease the intra-cluster open probability.

9. Global allosteric reorganization associated with desensitization

As expected for an allosteric process, the constriction of the desensitization gate occurs in concert with a global reorganization of the protein structure. So far, several local motions have been inferred from a variety of experimental approaches: 1) at the bottom of the TMD, the marked phenotypes of mutations at the interfaces between the M2 and M3 helices suggest that important reorganizations concern the ring of helices adjacent to M2; 2) at the opposite

end of the pore, X-ray crystal structures of pLGICs in a putative desensitized state also suggest that the upper part of the pore widens during desensitization. Fully consistent with that idea, nuclear magnetic resonance measurements made on the prokaryotic ELIC suggest both that the intracellular end of the pore constricts, and that its extracellular end expands during desensitization (Kinde et al., 2015).

Such movement of the extracellular end of the TMD is further expected to involve ECD-TMD interface rearrangements during desensitization. Several lines of evidence support this idea. First, marked changes in desensitization kinetics are observed upon mutation at this level (Bouzat et al., 2008; Zhang et al., 2011; reviewed in Zhang et al., 2013). Second, photoaffinity labelling experiments performed on *Torpedo* nAChRs revealed a differential labelling at the ECD-TMD interface of the δ subunit in the resting, active and desensitized states (Yamodo et al., 2010). Third, voltage-clamp fluorometry experiments on the $\alpha 1$ GlyRs show that variations in the fluorescence signal parallel the time course of desensitization onset when the fluorescent reporter is introduced at specific positions of the ECD-TMD interface. In contrast, when introduced higher up in the ECD, fluorescence does not report the active to desensitized transition (Wang and Lynch, 2011), suggesting that the ECD remains in a similar conformation in the active and desensitized states. Such a mechanism implies that the conformation of the orthosteric site, and thus the intrinsic affinity for the agonist, would be similar in the active and desensitized states, as previously proposed in various kinetic schemes (Auerbach and Akk, 1998; Edelstein et al., 1996). It should be noted here that the ECD conformation of the $\alpha 4\beta 2$ nAChR in a putative desensitized state differs significantly from the ECD conformation of the $\beta 3$ GABA_AR, showing a distinct degree of ECD twist. This led Hibbs and colleagues to propose that the $\beta 3$ GABA_AR structure reflects a partially desensitized state, while the $\alpha 4\beta 2$ nAChR structure would correspond to a fully desensitized state (Morales-Perez et al., 2016). However, it remains possible that such differential ECD conformations reflect a fundamental difference between nAChRs and anionic pLGICs in their ECD unbloomed states in general. Interpreting distinct structural conformations as distinct functional states would require the comparison of such conformations obtained on the same receptor, and future work is required to understand whether distinct desensitized states of a given pLGIC might differ in their ECD conformation.

10. Towards a full transition pathway of desensitization?

All of the above-mentioned symmetrical structures are probably relevant to the most stable slow desensitized states. However, the multiple temporal components of desensitization underlie the occurrence of a cascade of conformational changes. One extreme case could stem from concerted rearrangements of all subunits into distinct symmetrical desensitized conformations. At the other end of the spectrum, one could speculate that each subunit rearranges independently during desensitization. In such hypothesis, the various components of desensitization time constants could reflect the entry into various asymmetrical states, each subunit displaying a potentially distinct set of microscopic desensitization rate constants (Prince and Sine, 1999; Yamodo et al., 2010; Kinde et al., 2015). Such a scheme could account for multiphasic desensitization decay of heteromeric receptors, and even for

homomeric pLGICs (see Figure 11). One key parameter in this model is actually the number of subunits required to be in their desensitized state in order to prevent the ionic flow. Investigation of such speculative model would necessitate further work, although some evidence suggests that functional desensitization requires a conformational change at either one or two subunits in $\alpha 7$ nAChRs (daCosta and Sine, 2013).

11. Pharmacological modulation of desensitization

Desensitization provides an intrinsic second order regulatory mechanism of the activity of pLGICs, potentially endowing them with additional possibilities of neuromodulation in physiological conditions (Heidmann and Changeux, 1982). In particular, desensitization appears well-suited to affect pLGIC signalling during volume transmission, which involves low tonic concentrations of neurotransmitters (Vizi et al., 2010; Trueta and De-Miguel, 2012). For instance, a significant proportion of $\alpha 7$ nAChRs are found extrasynaptically, at remote distance from the locus of ACh release (Brumwell et al., 2002; Jones and Wonnacott, 2004), in both neuronal and non-neuronal microglial cells and astrocytes (Shytle et al., 2004; Duffy et al., 2011). However, $\alpha 7$ nAChRs display the fastest desensitization among pLGICs, since they desensitize fully within ~ 1 -100 milliseconds (see Box 1 for the discussion of variability, and Bouzat et al., 2017 for review). Most agonist-bound extrasynaptic $\alpha 7$ nAChR should thus be massively desensitized during volume transmission. Interestingly, a metabotropic role of $\alpha 7$ nAChRs has been proposed (King and Kabbani, 2016); an attractive hypothesis would be that such signalling could occur from the desensitized state, in the absence of any ionic flow.

From a pharmacological point of view, the $\alpha 7$ nAChRs are particularly interesting, since they are the target of a series of allosteric effectors, that bind at the TMD and display a large spectrum of pharmacological activities (Bouzat et al., 2017): 1) type I PAMs potentiate the peak response to ACh while minimally affecting desensitization; 2) type II PAMs cause a massive potentiation of $\alpha 7$ nAChRs currents while preventing their desensitization; 3) allosteric activators produce a non-desensitizing response in the absence of orthosteric agonists; 4) negative allosteric modulators (NAM) inhibit the response, although we don't currently know if they favour a desensitized state or another shut state; and 5) silent allosteric modulators (SAMs) don't affect the ACh-elicited current, but can competitively displace previously mentioned PAMs or NAMs. Given that subtle atomic differences can convert a PAM into a NAM or a SAM (Gill-Thind et al., 2015), it is likely that these molecules bind into the same site. Site-directed mutagenesis data support that this site is located in the TMD (Young et al., 2008; daCosta et al., 2011), and recent 3D models support the idea that $\alpha 7$ allosteric modulators bind in the vicinity of the desensitization gate (Newcombe et al., 2017). However, the precise location of the binding site of $\alpha 7$ allosteric modulators within the 3D structure remains to be established. Such detailed understanding could be of great therapeutic interest: animal studies have highlighted the potential of type II PAMs of $\alpha 7$ nAChRs in schizophrenia (Hurst, 2005), ischemia (Kalappa et al., 2013) and cognitive enhancement (Callahan et al., 2013). Alzheimer's disease being characterized by both cognitive decline and neuroinflammation, the combination of neuroprotective and procognitive properties makes

these molecules potential candidates in the treatment of this debilitating neurodegenerative disease (Bouzat et al., 2017).

Besides nAChRs, modulation of desensitization by endogenous compounds might also affect the signalling properties of other pLGICs, like the GABA_ARs. Indeed, these key players of the excitation-inhibition balance in the brain of vertebrates are the target of neurosteroids, which act as endogenous allosteric modulators. The two previously mentioned GLIC-(GABA_A α 1) and (GABA_A β 3)-(GABA_A α 5) chimeras were actually constructed in order to provide a structural platform for the analysis of the neurosteroid modulation. The binding site of potentiating neurosteroids is located at the bottom end of the TMD, at the intracellular end of the groove between the M3 and the M1 segments of adjacent subunits (Lavery et al., 2017; Miller et al., 2017), while inhibitory neurosteroids likely bind in an intra-subunit site, at the intracellular end of the M3/M4 interface (Lavery et al., 2017). Given that these sites are in the vicinity of the desensitization gate, one could expect that neurosteroids impact desensitization. Interestingly, previous work suggests that the potentiating neurosteroid THDOC slows down the recovery from desensitization of native GABA_ARs from cerebellar granule cells, while leaving the desensitization on-rate kinetics unaffected (Zhu and Vicini, 1997). However, the main effect of potentiating neurosteroids is to enhance the gating efficacy of GABA_ARs, leading to an increase of single channel activity under low GABA concentrations (Twyman and Macdonald, 1992), and to the increased macroscopic efficacy of partial agonists (Bianchi and Macdonald, 2003). These results might indicate that potentiating neurosteroids stabilize both the open and desensitized states over the resting state, leaving the microscopic desensitization rates unaffected. On the other hand, the inhibitory neurosteroid pregnenolone sulfate (PS) has been suggested to increase the desensitization rate of GABA_ARs (Shen et al., 2000). However, PS binding to GABA_ARs is state-dependent (Eisenman et al., 2003), complicating the macroscopic analysis of PS inhibition during co-application of GABA_AR agonists and PS. Still, single channel recordings show that PS shortens the duration of single-channel clusters of α 1 β 2 γ 2 GABA_ARs while minimally affecting the intra-cluster open probability (Akk et al., 2001). This would be fully consistent with PS exerting its inhibitory effects by enhancing GABA_ARs' desensitization.

On a more general note, drugs affecting the desensitization, or DAMs (desensitization-modifying allosteric modulators) of ligand-gated ion channels might hold significant therapeutic promises. Indeed, like all allosteric modulators, they would respect the “biological rhythms” of the receptors by only fine-tuning their response to specific physiological patterns of endogenous agonist release. Moreover, allosteric binding sites are much less conserved than the critical orthosteric sites: consequently, designing subtype-selective allosteric drugs is much easier than designing subtype-selective orthosteric ligands. For these two reasons, allosteric modulators should yield significantly broader therapeutic windows than orthosteric ligands or even allosteric activators, which can activate the receptors in the absence of orthosteric agonists. One particular well-known illustration is the benzodiazepine class of drugs: these compounds potentiate GABA_ARs by increasing their apparent affinity for GABA (Gielen et al., 2012), and they have replaced barbiturates in most prescriptions due to the toxicity of this latter class of molecules, which can directly activate GABA_ARs (Mathers and Barker, 1980; Parker et al., 1986; Rho et al., 1996; López-Muñoz et al., 2005). Compared to

other allosteric modulators, those that specifically affect the desensitization of pLGICs might even display milder functional effects and thus safer therapeutic windows: desensitization occurring downstream of activation, DAMs should minimally affect the peak agonist-concentration curve, and should only modulate the activity level in the sustained presence of the agonist. Such effect could be particularly beneficial for the treatment of pathologies affecting high frequency release or abnormal extracellular tonic levels of neurotransmitters.

12. Comparison with other ion channels: high prevalence of a two-gate mechanism

The desensitization gate model for pLGICs (Fig. 12A) is reminiscent of the C-type slow inactivation of voltage-gated K^+ and Na^+ channels. Indeed, this slow inactivation is thought to involve the collapse of the pore P-loop, which shapes the selectivity filter (Fig. 11B; Cuello et al., 2010; Payandeh et al., 2012; Zhang et al., 2012; Pau et al., 2017; Li et al., 2017), at a remote distance from the activation gate facing the intracellular end of the channel. Such model has been proposed initially for the prototypical voltage-gated Shaker potassium channel and the prokaryotic KcsA channel, although it has also been shown to be responsible for the run-down of distantly related TRPM2 channels (Toth and Csanady, 2012). Still, some caution needs to be exerted before generalizing: the analysis of pore-blocker kinetics suggests that the prokaryotic MthK potassium channel only has one gate located at the selectivity filter level, the canonical activation gate being constitutively in its open conformation (Posson et al., 2013). Early observations that led to the C-type inactivation model included the location of inactivation-enhancing mutations surrounding the P-loop (López-Barneo et al., 1993; Kurata and Fedida, 2006), as well as the effect of pore-blockers, which bind at the level of the selectivity filter and prevent desensitization by a foot-in-the-door mechanism (Choi et al., 1991; Kurata and Fedida, 2006). This provides an interesting parallel to the desensitization-enhancing effects of GABA_AR and GlyR mutations at the intracellular end of the M2/M3 interface, as well as the effects of picrotoxin, which is thought to prevent the collapse of the desensitization gate of anionic pLGICs (Gielen et al., 2015). Such similarities might seem surprising, given that pLGICs and voltage-gated channels adopt totally unrelated structural organizations: the latter are tetramers, whose core pore-forming domain comprises two transmembrane helices surrounding the re-entrant P-loop domain. It thus appears that structurally unrelated ion channels have converged towards a mechanism in which, after the activation through the opening of an activation gate, a topologically distinct desensitization/inactivation gate has been selected to limit ion flow under the sustained presence of the activating stimulus (Fig. 12A&B). Such functional convergence might be extended to other classes of ion channels, including the trimeric ATP-gated P2X channels. Indeed, the X-ray crystal structure of the human P2X₃ receptors has been solved recently in three different conformations, presumably reflecting the resting, active and desensitized states of the receptor (Fig. 12C; Mansoor et al., 2016). P2X₃ activation involves the stretching of the top half of the pore-lining α helices: the transition into a 3_{10} helical pitch produces a kink, which results in the opening of the channel, and which is stabilized by an intracellular cap domain. Upon cap unfolding, desensitization would involve the recoiling of the pore-lining helices, albeit in a different conformation compared to the resting state (Fig. 12C; Mansoor et

al., 2016). Of note, the extracellular ATP-binding domain of P2X₃ receptors remains in the same conformation in the active and desensitized states.

This dual gate model for the activation and desensitization/inactivation of ion channels has a potential major outlier: the family of ionotropic glutamate receptors (iGluRs), which mediate fast glutamatergic neurotransmission in the central nervous system of vertebrates. They comprise the fast-desensitizing kainate and AMPA receptors, whose activation kinetics are fast enough to follow trains of glutamate release occurring during high frequency stimulations (Attwell and Gibb, 2005), and the NMDA receptors, which require the binding of both glutamate and glycine for measurable activation (Johnson and Ascher, 1987; Clements and Westbrook, 1991). These tetrameric glutamate-gated receptors adopt very different structural topologies and activation mechanisms compared to pLGICs (Smart and Paoletti, 2012; Plested, 2016): each subunit is composed of two extracellular domains, namely the N-terminal domain (NTD) and the agonist binding domain (ABD), one transmembrane domain (TMD) resembling an inverted potassium channel, and one C-terminal cytoplasmic domain involved in the trafficking of the receptors at the plasma membrane. The NTD and the ABD are clamshell-like bilobed domains, the latter binding the agonist in its interlobe cleft. The agonist-elicited closure of individual ABDs is then directly coupled to the opening of the TMD. Almost two decades of functional and structural work have revealed that most, if not all, structural determinants of the desensitization of kainate and AMPA receptors are located in their extracellular part. Indeed, desensitization involves the dissociation of ABD dimers and a complete rearrangement of the extracellular architecture of kainate and AMPA receptors. Such dissociation would relieve the constraint exerted by the agonist-bound ABD on the TMD, allowing the pore to shut in a seemingly resting-like conformation (Fig. 12D; Sun et al., 2002; Dawe et al., 2013; Meyerson et al., 2014, 2016; Plested, 2016). Similar structural rearrangements also occur at NMDARs during their inhibition by allosteric modulators binding to the NTD of glutamate-binding subunits (Gielen et al., 2008; Zhu et al., 2016).

In this iGluR desensitization scheme, the pore might adopt only two possible conformations, either an open conformation in the active state, or a shut conformation identical in the resting and desensitized states. However, several points need to be considered before making any firm conclusion. First, the resolution of recent iGluR structures might be too low in some parts of the TMD to fully discard potential slight differences in the resting and desensitized states. Interestingly, recent cryo-EM data with higher resolution highlighted the structure of the channel open-state of the AMPA receptor, revealing the existence of a conformational change at the selectivity filter during activation (Twomey et al., 2017). This selectivity filter is constricted in the resting and desensitized states, thereby providing a secondary gate, which suggests that a two-gate mechanism might occur at iGluRs. Second, these cryo-EM structures are performed on iGluRs deleted for their cytoplasmic domain, which, in association with the detergent solubilisation, might affect the differential stability of various pore conformations. Third, a structural identity between the resting and desensitized states of kainate receptors might appear contradictory with some literature highlighting a metabotropic role of kainate receptors. Owing to such metabotropic role, kainate receptors can modulate GABA release by CA1 interneurons (Rodríguez-Moreno and Lerma, 1998) and can produce long-lasting

Desensitization of pentameric ligand-gated ion channels

inhibition of postspike potassium currents (I_{sAHP}) in CA1 pyramidal cells (Melyan et al., 2002) in a PKC-dependent manner, independently of any ionic flow. The dependency of metabotropic signalling on agonist concentration seems to involve the desensitized state(s) of the receptors: the kainate-induced inhibition of I_{sAHP} occurs with a kainate IC_{50} of ~ 15 nM in the pyramidal cells, which express GluK2-containing kainate receptors (Melyan et al., 2002). Such concentration is consistent with the apparent kainate affinity for the desensitized state of recombinant GluK2 kainate receptors expressed in HEK cells ($IC_{50} \sim 31$ nM; Jones et al., 1997). In the hypothesis that the metabotropic signalling of kainate receptors is transduced through their desensitized state, it would be expected that the desensitized and resting states differ in their intracellular conformations, thus requiring a differential TMD conformation. Last but not least, NMDA receptors can undergo some desensitization (Sather et al., 1992), albeit usually much slower and more limited than at AMPA and kainate receptors, through a calcium-dependent phosphorylation by calcineurine (Tong and Jahr, 1994; Tong et al., 1995). Recent work suggests that the pore-blockers ketamine and memantine differentially impact the desensitization of NMDA receptors, hinting towards a two-gate desensitization mechanism in this subfamily of iGluRs (Glasgow et al., 2017). The dual gate model for the activation and desensitization/inactivation of ion channels might thus be the rule rather than the exception.

Box 1. The variability of desensitization

1. Variability of outside-out patch-clamp recordings

One hallmark of the pLGICs' desensitization lies in its variability, which adds to the difficulty of investigating this process. Indeed, the kinetics of desensitization, as measured with fast theta-tube applications to outside-out patches, show high variability for the muscle-type nAChRs, GABA_ARs and GlyRs (Papke and Grosman, 2014; Papke et al., 2011). This variability of desensitization kinetics is particularly prominent at $\alpha 1$ GlyRs patches, some of which being well described by two- or four-components fits, all patches including a fast 5 ms component, and most of them including an intermediate 100 ms component (Papke and Grosman, 2014). Since outside-out recordings can be viewed as highly-dialyzed miniature whole-cell patch-clamp recordings, it is intriguing that such observation is mirrored by intra-cell variability when performing the whole-cell patch-clamp recordings: the desensitization kinetics and the extent of desensitization increase over time after entering the whole-cell configuration (unpublished personal observation at $\alpha 1\beta 2$ GABA_ARs; see also Papke et al., 2011 for time-dependent changes in the desensitization on-rates in outside-out patches). Unfortunately, the source for this huge variability is currently unknown (see below), which has considerably hampered research efforts to investigate the mechanisms of pLGICs' desensitization.

2. Discrepancy in desensitization kinetics between outside-out patch-clamp recordings and two-electrode voltage-clamp recordings

When expressing GABA_ARs and GlyRs in *Xenopus laevis* oocytes, the observed desensitization kinetics measured by two-electrode voltage clamp (TEVC) are much slower and less variable than the ones measured by outside-out patch-clamp recordings when expressing the same receptors in HEK or CHO cells: the fastest component for desensitization of $\alpha 1\beta 2\gamma 2$ GABA_ARs and $\alpha 1$ GlyRs are about 1.6 s and 1 s when measured by TEVC, respectively, and only account for 10-20% of the overall desensitization (Gielen et al., 2015). In contrast, outside-out patches pulled from HEK cells expressing $\alpha 1\beta 2\gamma 2$ GABA_ARs and $\alpha 1$ GlyRs usually show two fast components in the 3-5 ms and 70-100 ms range, which account together for ~70-75% of the desensitization amplitude (Papke et al., 2011). Such apparent discrepancy is usually explained by the intrinsic limitation of TEVC recordings of *Xenopus laevis* oocytes: the currents are rate-limited by the solution exchange around the oocyte, which usually takes almost a second. Thus, if desensitization occurs on a much faster timescale, it could be entirely missed, and the peak currents recorded by TEVC should only reflect the equilibrium between active receptors and receptors in their fast-desensitized state(s). However, two lines of evidence provide some arguments against this view:

1) Using super-saturating concentrations of agonist, it is possible to elicit TEVC currents in *Xenopus laevis* oocytes with a 20-80% rise time of about 25 ms at GABA_ARs and GlyRs. In such case, a fast desensitization component could be recorded with a decay time constant of 75 ms at mutant $\alpha 1^{G256V}$ GlyRs (Gielen et al., 2015), and a 70-100 ms component

present at wild-type $\alpha 1$ GlyRs should have been recorded, even if its amplitude would have been lowered compared to systems with a faster perfusion (Karlsson et al., 2011);

2) If we assume that most of the peak current is missed in TEVC recordings of *Xenopus laevis* oocytes because of desensitization, the apparent affinity for the agonist should be higher in TEVC recordings than in patch-clamp recordings of small cells. The opposite is actually observed: $\alpha 1\beta 2\gamma 2$ GABA_ARs expressed in HEK, which do show prominent desensitization, display an EC₅₀ for GABA in the 5-10 μ M range (Mortensen et al., 2004, 2011; Hernandez et al., 2017), while the same receptors expressed in *Xenopus laevis* oocytes lead to lower apparent affinities (EC₅₀ in the 40-150 μ M range depending on the $\gamma 2$ isoform; Downing et al., 2005; Campo-Soria et al., 2006; Gielen et al., 2012, 2015). This questions whether whole-cell patch-clamp recordings from small cells or outside-out patch-clamp recordings could actually change the pharmacological response of pLGICs, potentially by increasing apparent desensitization.

This discrepancy between outside-out and TEVC recordings is also observed at $\alpha 7$ neuronal nAChRs, which display an unusually fast and complete desensitization (Bouzat et al., 2017). Outside-out recordings performed with fast applications of ACh have been shown to result in currents decaying with a ~ 400 μ s desensitization time constant, which actually reflects the mean duration of single-channel open time as measured in cell-attached (non-dialysed) patches, i.e. ~ 350 μ s, suggesting that desensitization is so fast that it shapes the single-channel openings (Bouzat et al., 2008). Type 2 positive allosteric modulators (PAM), such as the prototypical PNU-120596 molecule (Hurst, 2005), can then produce a massive potentiation of single-channel activity by preventing desensitization (daCosta et al., 2011). In the absence of type 2 PAM, the desensitization kinetics of $\alpha 7$ nAChRs as measured in both outside-out and cell-attached patches should be far too fast to enable the detection of currents in TEVC recordings of *Xenopus laevis* oocytes. However, such recordings enable the detection of robust $\alpha 7$ nAChRs currents elicited by ACh alone, which desensitize with a time constant of ~ 100 ms. These currents elicited by ACh alone can amount to up to 10-20% of the current elicited by ACh in the presence of PNU-120596 (unpublished personal observation; see also Young et al., 2008). Such observations suggest that the desensitization of $\alpha 7$ nAChRs in *Xenopus laevis* oocytes measured in TEVC recordings is almost three orders of magnitude slower than the one measured in outside-out or cell-attached patches from HEK cells.

3. Basis of desensitization variability: a potential role for lipids?

When performing whole-cell patch-clamp recordings of HEK cells, one major effect lies in the dialysis of the intracellular medium – which is further enhanced in the outside-out patch-clamp conformation. It is thus possible that the dialysis of an intracellular component could be responsible for a gain of desensitization. In line with such hypothesis, the intracellular concentration of Ca²⁺ ions and the phosphorylation state of the receptors have been held responsible for modifying the desensitization rate of muscle-type nAChRs (Huganir and Greengard, 1990; Huganir et al., 1986), and phosphorylation of the GABA_AR $\beta 1$ ^{S409} serine residue by PKA has been shown to decrease the macroscopic desensitization rate of $\beta 1$ -containing GABA_ARs (Moss et al., 1992). The phosphorylation state cannot however account

for the extremely variable kinetics and extent of desensitization of GLIC expressed in HEK cells (Laha et al., 2013), since this prokaryotic receptor lacks the M3-M4 intracellular loop and is devoid of phosphorylation sites. Moreover, deleting most of the M3-M4 intracellular loop does not reduce the variability in the apparent rate of desensitization at $\alpha 1$ GlyR, arguing against a role of phosphorylation in this variability (Papke and Grosman, 2014).

An alternative hypothesis has been put forward in 2011, in which the fast macroscopic decline of GABA_ARs and GlyRs currents in patch-clamp experiments would not reflect actual desensitization of the receptors. Indeed, Karlsson et al. argued that such decline of current is actually due to the rather slow diffusion of chloride ions at the tip of the glass patch-clamp electrode, which results in a gradual loss of electrochemical driving force at the plasma membrane (Karlsson et al., 2011). In such hypothesis, the decline of current upon sustained activation is due to a diminished unitary current through the ion channels, and not to a desensitization-induced decrease in the receptors' open probability. Still, $\alpha 1\beta 2\gamma 2$ GABA_ARs display a cluster behaviour at the single-channel level (Mortensen et al., 2004), which is usually interpreted as desensitization. The duration of these clusters is in the 100 ms range at saturating GABA concentrations, suggesting that a fast component of desensitization on this timescale is inherent to patch-clamp recordings of $\alpha 1\beta 2\gamma 2$ GABA_ARs.

A third hypothesis would be that interactions with the glass pipettes might affect the distribution of lipids in the plasma membrane, these lipids playing a major role in the receptors' desensitization. Negatively charged lipids, in particular, could interact with the negatively charged surface of glass pipettes through the bridging by divalent cations such as calcium ions. In such hypothesis, it would then be relevant to note that the lipid composition of neurons can vary depending on the subcellular component (Calderon et al., 1995), and that different recombinant systems vary in that respect too (Opekarová and Tanner, 2003). Lipid candidates for such mechanism could include the phospholipid PIP₂, which is known, amongst other ion channel regulations, to gate inwardly rectifying potassium channels (Hansen et al., 2011), and to be required for the ivermectin-elicited gating of GIRK channels (Chen et al., 2017); PIP₂ depletion also leads to the desensitization of TRPV1 receptors (Yao and Qin, 2009). Interestingly, PIP₂ is a component of the inner leaflet of the plasma membrane, and thus ideally located to interact with the desensitization gate. If this hypothesis was true, it is important to note that cell-attached single-channel recordings would also likely be affected, e.g. that the duration of single-channel clusters may actually be decreased due to interactions between the glass pipette and the plasma membrane.

Box 2. Pore-blockers as allosteric modulators differentially stabilizing distinct states of the channel

Pore-blockers have proven useful pharmacological tools to discriminate between the various allosteric states of the channel. In cases where the binding site for a given pore-blocker displays a state-dependent conformation, the allosteric states of the channel will impact the affinity for the pore-blocker. The examples are plentiful in the pLGICs literature, such as picrotoxin, which prevents the desensitization of anionic pLGICs (see Main Text). This conclusion is actually reminiscent of experiments performed with another pore blocker, TBPS: the binding of radiolabelled TBPS to GABA_ARs is decreased under desensitizing conditions (Othman et al., 2012).

Pore-blockers have been used historically to study allosteric transitions at muscle-type nAChRs; tetracaine preferentially binds to agonist-unbound resting compared to agonist-bound desensitized states (Middleton et al., 1999), which shows that these two states are distinct. On the other hand, the pore-blocker chlorpromazine binds with high association on-rates to the open state of nAChRs, but rapid chlorpromazine binding is prevented under desensitizing conditions (Heidmann and Changeux, 1984, 1986). This result is all the more interesting since chlorpromazine binding occurs quite deep in the pore, with an involvement of M2 2' and 6' residues (Giraudat et al., 1986; Revah et al., 1990; Chiara et al., 2009). It is thus tempting to speculate that chlorpromazine acts on nAChRs in a similar manner as picrotoxin acts at anionic pLGICs, with the binding of this pore-blocker competing with the closure of a desensitization gate.

More recently, the pore-blocking properties of choline at muscle-type nAChRs gave credence to the two-gate model proposed by Auerbach & Akk: choline induces longer single-channel openings, while leaving the desensitization properties unaffected. This led to the conclusion that choline-binding in the pore interferes with an activation gate, while leaving the desensitization gate unaffected, and thus that these two molecular entities are distinct (Purohit and Grosman, 2006). Nevertheless, another recent study suggests on the contrary that the binding of choline has only minimal effect on the closing rate – i.e. on the duration of single-channel openings (Lape et al., 2009). Further work is required to fully understand the interactions between choline and the pore of nAChRs in their different functional states.

This use of pore-blockers is not restricted to the study of pLGICs: tetraethylammonium binds at the level of the selectivity filter of potassium channels and prevents slow inactivation by a foot-in-the-door mechanism (Choi et al., 1991; Kurata and Fedida, 2006), while ketamine and memantine differentially affect the desensitization of NMDA receptors (Glasgow et al., 2017).

Pore-blockers thus don't only act as mere plugs, and their state-dependent affinity might even be used to design clinically relevant drugs, e.g. to target preferentially extrasynaptic receptors over synaptic ones, as proposed for the action of memantine at NMDA receptors (Xia et al., 2010).

Figure legends

Abstract Figure. Desensitization of pentameric ligand gated ion channels involves a desensitization gate distinct from the activation gate. A virtual macroscopic electrophysiological trace highlights the activation and desensitization of pLGICs. In the absence of agonist, the receptors are in their resting conformation, while agonist application elicits an electrophysiological current by promoting the occupancy of open state. Upon prolonged application, the agonist-bound receptors transit from their open-channel active state to a shut-channel state refractory to any activation, i.e. the desensitized state. Of note, a small fraction of receptors can be active in the absence of the agonist (unliganded openings, extremely rare at wild type pLGICs), and the peak current reflects an equilibrium between the resting and the active states, which depends on the open probability of the receptor. Moreover, the steady-state current upon sustained agonist application, which varies in amplitude throughout the pLGIC family, reflects the thermodynamic equilibrium between the active and desensitized states. Schematic depictions of pLGICs' conformations are shown for two simplified subunits, in which only the M2 pore-lining is portrayed for the transmembrane domain. The upper half of the pore is shut in the resting state, and activation involves the contraction and the rotation of extracellular domains ("unblooming" and "twisting"), which stabilizes the open-pore conformation. Finally, desensitization involves the closure of a gate located at the intracellular end of the pore. This structural rearrangement is accompanied by a widening of the upper half of the pore, while the extracellular domain might remain in the same conformation as in the active state.

Figure 1. Structural overview and gating mechanism of pLGICs. *A, Left*, Top view of GluCl bound to glutamate (pdb code 3RIF; Hibbs and Gouaux, 2011). One subunit is highlighted in green, coordinating a glutamate molecule shown in orange at its principal face. Note the M2 helices from all five subunits, which line the ion conducting pore. *Right*, Side view of GluCl, which delimits the extracellular domain (ECD) in the extracellular space (Ext.) and the transmembrane domain (TMD). The plasma membrane is schematized in yellow. Note the absence of the intracellular domain (ICD) in the intracellular space (Int.) for this particular construct. *B*, Schematic depiction of pLGICs' activation. For the sake of clarity, only two simplified subunits are shown, omitting the M1, M3 and M4 segments of each subunit to retain only the M2 pore-lining segments. In this scheme, the agonist (orange oval shape) binds to its ECD interfacial orthosteric site, which elicits a pre-activation or "priming" of the receptor by promoting an unbloomed conformation of the ECD. In other words, the primed conformation displays a higher affinity for the agonist than the resting conformation. The final activation step results from the opening of the channel gate, in the upper half of the pore, potentially concomitant with the twisting of the entire receptor. Please note that this scheme is oversimplified, and does not address well-known features of pLGICs activation, such as the multiplicity of agonist binding sites, nor does it distinguish between flipping, priming or catch and hold mechanisms.

Figure 2. Location of molecular determinants of anionic pLGICs' desensitization in the lower half of the TMD. *Top left*, Top view of the TMD of GluCl (pdb code 3RI5; Hibbs and Gouaux, 2011). One subunit is highlighted in green, showing the arrangement of transmembrane segments M1-M4 respectively to the pore: M4 is the most distal segment, while M2 forms the pore-lining α helix. The other subunits are coloured in grey. *Top right*, Enlargement showing the proximity of the M3 and M1 helices of adjacent subunits. *Bottom right*, Side view depicting the location of the M1-M2 linker, in the vicinity of the intracellular end of the M3 helix from the adjacent subunit. Note also that the cytoplasmic M3-M4 loop extends at the C-terminal end of M3. *Bottom left*, Rotated side view of the M2 and M3 segments of the subunit coloured in green. The M2 9' and -2' residues, part of the activation gate and the selectivity filter respectively, are shown in stick representation. Their mutation affects the gating and desensitization of pLGICs (see Main Text). Residues highlighted with the sphere representation are homologous to the residues whose mutation strongly modulate the desensitization of $\alpha 1\beta 2$ GABA_ARs, $\alpha 1\beta 2\gamma 2$ GABA_ARs and $\alpha 1$ GlyRs in Gielen et al., 2015. Numbering of residues has been made according to Jaiteh et al., 2016.

Figure 3. Picrotoxin prevents the desensitization of $\alpha 1$ GlyRs. *A*, Side view of the M2 segments from GluCl (pdb code 3RI5), showing only two distal subunits for clarity. Picrotoxin (PTX) binding site is delimited by the -2' and 2' residues, shown in sticks. The 9' residue position serves as a reference to pinpoint the bottom end of the activation gate. The 4' and -3' residues delineate the bottom of the M2/M3 interface, which bears critical determinants of the desensitization of anionic pLGICs (see Main Text and Fig. 2). *B*, Depiction of a scheme, in which desensitization of anionic pLGICs involves a desensitization gate overlapping the PTX binding site. Binding of PTX thus prevents the entry into the desensitized state. Moreover, PTX cannot associate to or dissociate from the resting state of the pore. This is fully consistent with previous studies, which showed that picrotoxin is trapped in the resting state of the receptor (Bali and Akabas, 2007), under the activation gate (Hibbs and Gouaux, 2011; Rossokhin and Zhorov, 2016). *C*, Two-electrode voltage clamp (TEVC) recording from an oocyte expressing $\alpha 1$ GlyRs. Supersaturating glycine (10 mM) elicits a current that desensitizes over a two-minutes long application. This current can be blocked by PTX (500 μ M). Co-application of glycine and PTX for three minutes, allowing equilibration between the various allosteric states, yields a pronounced rebound current upon wash-out of PTX. Data taken from Gielen et al., 2015. *D*, Kinetic model corresponding to the scheme depicted in panel B. The receptor can be found in its agonist-free resting state (R), and in agonist-bound resting (AR), open (AO) or desensitized (AD) states. P denotes PTX-bound states. Except for ρ , all values are taken from Gielen et al., 2015; ρ values greater than one reflect the stabilization of the resting state by PTX. It should be noted here that our model does not address many fine aspects of pLGICs' gating: 1) Only one agonist binding site was included, whereas pLGICs usually require the binding of two or three agonist molecules for full activation (Lape et al., 2008; Rayes et al., 2009; Corradi et al., 2009; Gielen et al., 2012). No pre-activation step is included either. Fine details of receptors' activation by low concentrations of agonists (or by partial agonists) would not be recapitulated in our model; 2) Channel opening requires the binding of the agonist in our model, while it is well known that

unliganded pLGICs can spontaneously open. Such spontaneous gating is however extremely rare at wild type pLGICs (Purohit and Auerbach, 2009), which is the reason why we decided not to include it; 3) Our scheme for agonist binding, activation and subsequent desensitization is linear, the agonist being thus unable to dissociate from the desensitized state in our model. This is in contradiction with what is known from desensitization recovery, and our model thus couldn't reflect what happens during desensitization recovery in the absence of the agonist, for example during the wash-out of a desensitizing application of agonists; 4) Only one desensitized state is included, corresponding to a slow component of desensitization. Accounting for the detailed multiphasic components of desensitization is thus out of reach in our model. **E**, Kinetic model, in which the PTX-bound receptor can desensitize (ADP state). PTX is trapped in the desensitized state, akin what happens in the resting state. Such scheme would reflect the hypothesis that desensitization and activation might involve the same physical gate. All rates are kept identical to the ones from panel D. **F**, Simulations performed with the kinetic model from panel D, for ρ values of 1 (grey trace), 10 (blue trace) and 100 (red trace). Note the simulations with ρ values of 1 and 10 display pronounced rebound currents akin the one seen in experiments. Note also that further increase in ρ leads to slower apparent recovery of the current upon PTX wash-out, and to a much reduced rebound current (see Main Text for discussion). Simulations were performed with QuB (Nicolai and Sachs, 2013). **G**, Simulations performed with the kinetic model from panel E, for ρ values of 1 (grey trace), 10 (blue trace) and 100 (red trace). None of these simulations can recapitulate the pronounced experimental rebound current.

Figure 4. Interplay between ivermectin and picrotoxinin at zebrafish $\alpha 1$ GlyR: a plausible kinetic scheme. **A**, Kinetic scheme proposed for the dual modulation of the zebrafish $\alpha 1$ GlyR, whose cryo-EM structure was solved in Du et al., 2015. In this model, the binding of the agonist glycine (A) to the receptor (R) promotes its transition to the glycine-bound active state (AO), which can subsequently desensitize (AD). Ivermectin (Iv) is hypothesized to stabilize the open state over the resting state, without affecting the receptor's microscopic desensitization: Iv increases the opening rate β by a factor γ , and decreases the shutting rate by a factor δ . Picrotoxinin (P) acts accordingly to Fig. 3D: it prevents desensitization and promotes the resting state of the receptor by decreasing the opening rate of the channel by a factor ϵ . Note that the active state of receptors bound to glycine alone or to glycine and ivermectin are the sole ion conducting states (other states being either inactive or blocked by picrotoxinin). These two states are boxed in green. Note also that the effects of ivermectin and picrotoxinin are fully additive: when bound to both ivermectin and picrotoxinin, the channel has a microscopic opening rate of $\beta \cdot \gamma / \epsilon$, and a microscopic shutting rate given by α / δ . Such hypothesis precludes any direct interaction between these two modulators. Finally, this kinetic model does not aim at portraying all features of GlyR functioning (see Fig. 3D legend). **B**, Parameters used for kinetic simulations based on the scheme from panel A. Note that these parameters were chosen arbitrarily – their exact values have not been determined for the zebrafish $\alpha 1$ GlyR crystallized construct. The only constraints were to satisfy a peak apparent glycine affinity of 0.26 mM, and to provide a macroscopic desensitization profile comparable to the one from Du et al., 2015. **C**, Simulation based on the kinetic model and parameters from panels A and B. Currents elicited by 0.3 mM

glycine alone are inhibited up to ~90% by 1 mM picrotoxinin (PTX), and are potentiated approximately two-fold by 5 μ M ivermectin. Note that currents elicited by co-application of glycine and ivermectin are inhibited by picrotoxinin by only ~20%. **D**, Simulation indicating that, with the kinetic model and parameters from panels A and B, the application of 10 mM glycine (trace in grey) elicits the same peak current and the same desensitization as the co-application of 0.3 mM glycine and 5 μ M ivermectin.

Figure 5. Structural rearrangements at the level of the selectivity filter and the activation gate during desensitization. *A, Left*, Side view of the M2 segments from the presumably open states (O) of GLIC (coloured in red; pdb code 4HFI) and the *C. elegans* GluCl (coloured in light pink; pdb code 3RI5), superimposed with the presumably desensitized states (D) of the human α 3 GlyR (coloured in blue; pdb code 5TIN) and β 3 GABA_AR (coloured in light cyan; pdb code 4COF), showing only two distal subunits for clarity. Note the difference in the backbone conformations between the O and D structures. *Middle*, Top view of the pore at the level of M2 -2' residues (shown in sticks), which are part of the selectivity filter, for the structures mentioned above. Note the reduction in the pore diameter of D structures compared to O structures. *Right*, Top view of the pore at the level of 9' residues (shown in sticks), which are part of the activation gate, for the structures mentioned in panel A. Note the increase in the pore diameter of D structures compared to O structures, and the difference in the M2 9' side-chain orientations, which point towards the neighbouring M2 segments for D structures. **B, Left**, Side view of the M2 segments from the presumably open state (O) of GLIC and the presumably desensitized state (D) of the human α 3 GlyR, superimposed with the structure of the α 4 β 2 nAChR (coloured in green; pdb code 5KXI). *Middle*, Top view of the pore at the level of the selectivity filter. Note that it might be difficult to assign a functional status to the α 4 β 2 nAChR structure on this basis, especially when taking into account potential rotamers of the nAChR -1' glutamate (see Main Text). *Right*, Top view of the pore at the level of 9' residues (shown in sticks). Note that the conformation of the α 4 β 2 nAChR structure superimposes well to the α 3 GlyR in a putative desensitized state.

Figure 6. Proposed model for the gating and desensitization of pLGICs: a dual gate mechanism. Schematic depiction of pLGICs' activation and desensitization. It expands on the iconography from Figure 1B to include a desensitization step, in which the intracellular end of the pore constricts during desensitization, thus forming a physical desensitization gate distinct from the activation gate.

Figure 7. A theoretical model: an allosteric inhibitor selectively stabilizing an agonist-bound pre-active state would increase the apparent affinity for the agonist. *A*, Putative free energy diagram highlighting the effect of an allosteric inhibitor I, which would selectively stabilize the pre-active state of a receptor (F) over its resting (R) or active (O) states in the presence of the agonist (A). Note that the free energy of the AF state is decreased by δG in the presence of I. *B*, Translation of the free energy diagram from panel A into a linear kinetic model for the activation of the receptor by the agonist and its inhibition by I. In the presence of I, note the dependence of the pre-activation and activation microscopic rates

on the value of δG and those of δG^f and δG^o , the two latter reflecting the effect of the inhibitor's binding on the transition states during the $AR \rightarrow AF$ and the $AO \rightarrow AF$ transitions, respectively. **C**, Equilibrium constants for the $AR \leftrightarrow AF$ and $AF \leftrightarrow AO$ equilibria are noted F and E , respectively. Note that the value of those constants, in the presence of the inhibitor I , depends solely on two parameters: the value of the constants in the absence of I , and the value of δG . In other words, the value of the pre-activation and activation equilibrium constants do not depend on δG^f or δG^o . **D**, Expression of the maximal peak open probability ($P_{o,max}$) and of the apparent EC_{50} for the agonist ($EC_{50,A}$) in control condition and in the presence of a saturating concentration of the inhibitor I (see Gielen et al., 2012 for further details). The binding of I causes both a decrease in the open probability – meaning that I is indeed an inhibitor – and a decrease in the apparent agonist EC_{50} – in other words, I increases the apparent affinity for the agonist.

Figure 8. The selective stabilization of a pre-active state can recapitulate the effects of DHA on wild-type GLIC. **A**, Proposed kinetic model of wild-type GLIC, expanding on Fig. 7B and including a desensitization step to reach the agonist-bound desensitized state AD . For the sake of simplicity, the inhibitor DHA (I) is presumed to stabilize selectively the agonist-bound pre-active state AF by decreasing the $AF \rightarrow AR$ (f) and $AF \rightarrow AO$ (β) microscopic rates, although similar results would be obtained with modified f^+ and α rates, as long as the equilibrium constant f^+/f - and β/α are conserved. Note that the model probably oversimplifies many aspects of the gating of GLIC: for example, the model only contains one single binding site for protons and DHA, whereas the homomeric GLIC probably contains at least five proton binding sites, and harbours five DHA sites. Unliganded openings and proton dissociation from the desensitized state are not portrayed here, although they probably occur like for other pLGICs. **B**, Parameters for kinetic simulations of GLIC modulation by DHA. Note that the exact values for all the microscopic steps are unknown, and were chosen arbitrarily. **C**, Simulation of GLIC currents elicited by pH 4.5 applications, highlighting the inhibitory effect of DHA co-application, which increases the rate and the extent of current loss upon prolonged proton applications. This could be misinterpreted in terms of an increased rate of desensitization, but only reflects the slow on-rate of DHA association to GLIC in the kinetic model. **D**, Theoretical concentration-response curve for DHA inhibition in simulated currents. The effect of DHA co-application is assessed by its effect on the ratio between the steady-state and the peak current elicited by a pH 4.5 application. With such measurement, simulations yield an apparent DHA IC_{50} of $9.7 \mu M$. **E**, Simulation of GLIC currents elicited by increasing proton concentrations (pH 7.0 to pH 3.5), either in control conditions (black trace), or in the continued presence of $50 \mu M$ DHA (red trace). **F**, *Left*, Normalized concentration-response curve for the proton-elicited peak currents in control condition (plain black line, filled black circles; $pH_{50} = 5.0$) or in the continued presence of $50 \mu M$ DHA (plain red line, filled red triangles; $pH_{50} = 5.2$). *Right*, Normalized concentration-response curve for the proton-elicited steady-state currents in control condition (dashed black line, empty black circles; $pH_{50} = 5.2$) or in the continued presence of $50 \mu M$ DHA (dashed red line, empty red triangles; $pH_{50} = 5.6$). Note that DHA increases the apparent affinity for proton in these simulations, 1.6-fold and 4-fold in the cases of peak and steady-state responses, respectively.

Figure 9. The selective stabilization of a pre-active state can recapitulate the effects of DHA on GLIC 9' mutants. *A*, Free energy diagram highlighting the putative effect of the M2 9' I to A mutation on GLIC. In this model, the M2 9' mutation selectively stabilizes the open state (AO) over the resting (AR), pre-active (AF) and desensitized (AD) shut states (plain black line, compared to the wild type in dashed grey line). Two schemes are then considered to account for the DHA inhibition: in scheme I (blue line), the inhibitor DHA selectively stabilizes the desensitized state over all other states and decreases its free energy by δG_d ; whereas in scheme II (red line), the inhibitor DHA selectively stabilizes the pre-active state and decreases its free energy by δG_d . In both schemes, the effects of DHA and the M2 9' mutation are considered additive. *B*, *Left*, Translation of the free energy diagram from panel A into a linear kinetic model for the activation of GLIC by the agonist proton (A) and its inhibition by DHA. *Right*, Translation of the free energy effects of the M2 9' I to A mutation into kinetics effects, highlighting the increased efficacy of gating and the decreased equilibrium constant for desensitization. *C*, *Left*, In scheme I, DHA binding displaces the AO \leftrightarrow AD equilibrium towards the AD state. In other words, the affinity of GLIC for DHA is increased in the desensitized state. *Right*, In scheme II, DHA affects equally the AR \leftrightarrow AF and the AF \leftrightarrow AO equilibria, displacing them towards the AF state. In other words, the affinity of GLIC for DHA is increased in the pre-active state. *D*, Simulated GLIC currents elicited by pH 4.5 applications, highlighting the inhibitory effect of DHA co-application on wild type GLIC (black trace) in both scheme I (left) and scheme II (right). Assuming that the M2 9' mutation selectively stabilizes the open state, the inhibitory effect of DHA is predicted to be lost for the 9' GLIC mutant, both in scheme I (blue trace, left) and in scheme II (red trace, right). Parameters for the simulation are identical to Fig. 8B.

Figure 10. The inhibition of GLIC peak currents by pre-applications of DHA favours an effect of DHA on the pre-activation, rather than the desensitization, of GLIC. *A*, Wild type GLIC currents simulated according to scheme I from Fig. 9, i.e. with DHA promoting desensitization. Note that DHA pre-application fails to inhibit the peak current elicited by pH 4.5. *B*, Wild type GLIC currents simulated according to scheme II from Fig. 9, i.e. with DHA selectively stabilizing the pre-active state AF. Note that pre-application of 10 μ M and 50 μ M DHA inhibit the peak current elicited by pH 4.5 by 25% and 55%, respectively. All these simulations are performed with the same parameters as in Fig. 8B.

Figure 11. Independent transition of identical subunits into a unique desensitized state can result in multiphasic desensitization profiles in homomeric ligand-gated ion channels. *A*, In this illustrative model of a trimeric homomeric receptor (R) gated by an agonist (A), the agonist-bound receptor can activate (AO state), and each subunit can subsequently undergo desensitization. AD_{ij} denotes a state where subunits *i* and *j* are in their desensitized state. One major assumption of this model is that all subunits behave independently, i.e. the microscopic rates for the AO \leftrightarrow AD_i and AD_i \leftrightarrow AD_{ij} equilibria are the same regardless of the identity of subunits *i* and *j*, the desensitization on- and off-rates being noted d^+ and d^- , respectively. In other words, the desensitization state of one subunit does not influence the desensitization kinetics of another subunit. Finally, the pore is

considered as non-conducting, i.e. desensitized from a functional point of view, as soon as one single subunit has entered its desensitized state. As a result, only the AO state is conducting. **B**, Arbitrary parameters chosen for the kinetic model from panel A. **C**, *Left*, Simulation of currents based on the model and parameters from panel A & B, elicited by a saturating 10 mM application of agonist. *Middle and Right*, A one-component fit (dashed blue line) does not faithfully reproduce the simulated current (plain trace in grey), unlike a two-component fit (dashed red line). The slow component reflects the entry of receptors in states where several subunits have desensitized.

Figure 12. Desensitization and inactivation mechanisms across structurally unrelated families of ligand- and voltage-gated ion channels. See Main Text for full discussion. **A**, Schematic depiction of pLGICs' activation and desensitization. For the sake of clarity, only two simplified subunits are shown, omitting the M1, M3 and M4 segments of each subunit to retain only the M2 pore-lining segments in the transmembrane domain (TMD). Agonist binding occurs at the interface between two adjacent extracellular domains (ECD) and activation involves the opening of the pore in its upper half, while desensitization corresponds to the constriction of the desensitization gate at the level of the selectivity filter, at the intracellular end of the pore. Note the widening of the upper part of the pore during desensitization, which is probably accompanied by a rearrangement of the ECD-TMD interface. **B**, Schematic depiction of the slow C-type inactivation of tetrameric voltage-gated potassium and sodium channels. For clarity, only two subunits (or repeat domains in the case of eukaryotic sodium channels) are shown, and voltage-sensing domains are omitted. Activation is thought to open a gate at the intracellular end of the pore, while C-type inactivation presumably involves the collapse of the P-loop, which also forms the selectivity filter. Similar mechanisms have been suggested for the run-down of the structurally related ATP- and calcium-gated TRPM2 channel. **C**, Schematic depiction of human P2X₃ receptors' activation and desensitization. Similarly to pLGICs, these trimeric ATP-gated receptors bind their agonist at the interface between the ECDs of adjacent subunits. Activation of human P2X₃ receptors involves the stretching of the pore-lining TM2 helix, owing to a change in its helical pitch. This active state is stabilized by a cap domain. Unfolding of this cap domain presumably enables the recoiling of the TM2 segment into an α helix, thereby resulting in a desensitized state structurally distinct from the resting state at the pore level. **D**, Schematic depiction of ionotropic glutamate receptors' activation and desensitization. Here again, only two subunits are shown for clarity, out of four. The agonist binds to the interlobe cleft of the agonist binding domain (ABD) of individual domain, which results in the closure of this clamshell-like domain. Since the ABDs form dimers through their upper lobes, this closure results in an increased distance between the lower lobes, which are directly connected to the TMD. This movement results in the opening of the channel activation gate. Upon desensitization, the ABD dimers dissociate, which completely rearranges the ABD layer and releases the tension exerted on the pore in the active state. In this model, the TMD of iGluRs adopt the same conformation in the resting and desensitized states. Note that this model applies to the AMPA and kainate subfamilies of fast-desensitizing iGluRs. The desensitization of NMDA receptors might well depart from this view (see Main Text).

Desensitization of pentameric ligand-gated ion channels

References

- Akabas, M.H. (2013). Using molecular dynamics to elucidate the structural basis for function in pLGICs. *Proc. Natl. Acad. Sci. U. S. A.* *110*, 16700–16701.
- Akk, G., Bracamontes, J., and Steinbach, J.H. (2001). Pregnenolone sulfate block of GABA(A) receptors: mechanism and involvement of a residue in the M2 region of the alpha subunit. *J. Physiol.* *532*, 673–684.
- Althoff, T., Hibbs, R.E., Banerjee, S., and Gouaux, E. (2014). X-ray structures of GluCl in apo states reveal a gating mechanism of Cys-loop receptors. *Nature* *512*, 333–337.
- Attwell, D., and Gibb, A. (2005). Neuroenergetics and the kinetic design of excitatory synapses. *Nat. Rev. Neurosci.* *6*, 841–849.
- Auerbach, A., and Akk, G. (1998). Desensitization of mouse nicotinic acetylcholine receptor channels. A two-gate mechanism. *J. Gen. Physiol.* *112*, 181–197.
- Bali, M., and Akabas, M.H. (2007). The location of a closed channel gate in the GABAA receptor channel. *J. Gen. Physiol.* *129*, 145–159.
- Basak, S., Schmandt, N., Gicheru, Y., and Chakrapani, S. (2017). Crystal structure and dynamics of a lipid-induced potential desensitized-state of a pentameric ligand-gated channel. *ELife* *6*.
- Bianchi, M.T., and Macdonald, R.L. (2001). Mutation of the 9' leucine in the GABAA receptor γ 2L subunit produces an apparent decrease in desensitization by stabilizing open states without altering desensitized states. *Neuropharmacology* *41*, 737–744.
- Bianchi, M.T., and Macdonald, R.L. (2003). Neurosteroids shift partial agonist activation of GABA(A) receptor channels from low- to high-efficacy gating patterns. *J. Neurosci. Off. J. Soc. Neurosci.* *23*, 10934–10943.
- Bocquet, N., Prado de Carvalho, L., Cartaud, J., Neyton, J., Le Poupon, C., Taly, A., Grutter, T., Changeux, J.-P., and Corringer, P.-J. (2007). A prokaryotic proton-gated ion channel from the nicotinic acetylcholine receptor family. *Nature* *445*, 116–119.
- Bocquet, N., Nury, H., Baaden, M., Le Poupon, C., Changeux, J.-P., Delarue, M., and Corringer, P.-J. (2009). X-ray structure of a pentameric ligand-gated ion channel in an apparently open conformation. *Nature* *457*, 111–114.
- Bouzat, C., Bartos, M., Corradi, J., and Sine, S.M. (2008). The Interface between Extracellular and Transmembrane Domains of Homomeric Cys-Loop Receptors Governs Open-Channel Lifetime and Rate of Desensitization. *J. Neurosci.* *28*, 7808–7819.
- Bouzat, C., Lasala, M., Nielsen, B.E., Corradi, J., and Del Carmen Esandi, M. (2017). Molecular function of α 7 nicotinic receptors as drug targets. *J. Physiol.*
- Boyd, N.D., and Cohen, J.B. (1980). Kinetics of binding of [3H]acetylcholine and [3H]carbamoylcholine to Torpedo postsynaptic membranes: slow conformational transitions of the cholinergic receptor. *Biochemistry (Mosc.)* *19*, 5344–5353.
- Breitinger, H.-G., Lanig, H., Vohwinkel, C., Grewer, C., Breitinger, U., Clark, T., and Becker, C.-M. (2004). Molecular dynamics simulation links conformation of a pore-flanking region to hyperekplexia-related dysfunction of the inhibitory glycine receptor. *Chem. Biol.* *11*, 1339–1350.
- Brumwell, C.L., Johnson, J.L., and Jacob, M.H. (2002). Extrasynaptic alpha 7-nicotinic acetylcholine receptor expression in developing neurons is regulated by inputs, targets, and activity. *J. Neurosci. Off. J. Soc. Neurosci.* *22*, 8101–8109.
- Cachelin, A.B., and Colquhoun, D. (1989). Desensitization of the acetylcholine receptor of frog end-plates measured in a Vaseline-gap voltage clamp. *J. Physiol.* *415*, 159–188.
- Calderon, R.O., Attema, B., and DeVries, G.H. (1995). Lipid composition of neuronal cell bodies and neurites from cultured dorsal root ganglia. *J. Neurochem.* *64*, 424–429.
- Calimet, N., Simoes, M., Changeux, J.-P., Karplus, M., Taly, A., and Cecchini, M. (2013). A gating mechanism of pentameric ligand-gated ion channels. *Proc. Natl. Acad. Sci. U. S. A.* *110*, E3987–3996.
- Callahan, P.M., Hutchings, E.J., Kille, N.J., Chapman, J.M., and Terry, A.V. (2013). Positive allosteric modulator of alpha 7 nicotinic-acetylcholine receptors, PNU-120596 augments the effects of donepezil on learning and memory in aged rodents and non-human primates. *Neuropharmacology* *67*, 201–212.

Desensitization of pentameric ligand-gated ion channels

- Campo-Soria, C., Chang, Y., and Weiss, D.S. (2006). Mechanism of action of benzodiazepines on GABA_A receptors. *Br. J. Pharmacol.* *148*, 984–990.
- Cecchini, M., and Changeux, J.-P. (2015). The nicotinic acetylcholine receptor and its prokaryotic homologues: Structure, conformational transitions & allosteric modulation. *Neuropharmacology* *96*, 137–149.
- Chang, Y., and Weiss, D.S. (2002). Site-specific fluorescence reveals distinct structural changes with GABA receptor activation and antagonism. *Nat. Neurosci.* *5*, 1163–1168.
- Chang, Y., Ghansah, E., Chen, Y., Ye, J., Weiss, D.S., and Chang, Y. (2002). Desensitization mechanism of GABA receptors revealed by single oocyte binding and receptor function. *J. Neurosci. Off. J. Soc. Neurosci.* *22*, 7982–7990.
- Changeux, J.P. (1990). Functional Architecture and Dynamics of the Nicotinic Acetylcholine Receptor: An Allosteric Ligand-Gated Ion Channel. In *Fidia Research Foundation Neuroscience Award Lectures*, pp. 21–168.
- Chen, I.-S., Tateyama, M., Fukata, Y., Uesugi, M., and Kubo, Y. (2017). Ivermectin activates GIRK channels in a PIP₂-dependent, G $\beta\gamma$ -independent manner and an amino acid residue at the slide helix governs the activation. *J. Physiol.* *595*, 5895–5912.
- Chiara, D.C., Hamouda, A.K., Ziebell, M.R., Mejia, L.A., Garcia, G., and Cohen, J.B. (2009). [³H]Chlorpromazine Photolabeling of the *Torpedo* Nicotinic Acetylcholine Receptor Identifies Two State-Dependent Binding Sites in the Ion Channel. *Biochemistry (Mosc.)* *48*, 10066–10077.
- Choi, K.L., Aldrich, R.W., and Yellen, G. (1991). Tetraethylammonium blockade distinguishes two inactivation mechanisms in voltage-activated K⁺ channels. *Proc. Natl. Acad. Sci. U. S. A.* *88*, 5092–5095.
- Clements, J.D., and Westbrook, G.L. (1991). Activation kinetics reveal the number of glutamate and glycine binding sites on the N-methyl-D-aspartate receptor. *Neuron* *7*, 605–613.
- Colquhoun, D., and Lape, R. (2012). Allosteric coupling in ligand-gated ion channels. *J. Gen. Physiol.* *140*, 599–612.
- Corradi, J., Gumilar, F., and Bouzat, C. (2009). Single-Channel Kinetic Analysis for Activation and Desensitization of Homomeric 5-HT_{3A} Receptors. *Biophys. J.* *97*, 1335–1345.
- Corringer, P.J., Bertrand, S., Galzi, J.L., Devillers-Thiéry, A., Changeux, J.P., and Bertrand, D. (1999). Mutational analysis of the charge selectivity filter of the $\alpha 7$ nicotinic acetylcholine receptor. *Neuron* *22*, 831–843.
- Corringer, P.-J., Poitevin, F., Prevost, M.S., Sauguet, L., Delarue, M., and Changeux, J.-P. (2012). Structure and pharmacology of pentameric receptor channels: from bacteria to brain. *Struct. Lond. Engl.* *1993* *20*, 941–956.
- Cuello, L.G., Jogini, V., Cortes, D.M., and Perozo, E. (2010). Structural mechanism of C-type inactivation in K(+) channels. *Nature* *466*, 203–208.
- Cymes, G.D., and Grosman, C. (2011). Tunable pK_a values and the basis of opposite charge selectivities in nicotinic-type receptors. *Nature* *474*, 526–530.
- Cymes, G.D., and Grosman, C. (2016). Identifying the elusive link between amino acid sequence and charge selectivity in pentameric ligand-gated ion channels. *Proc. Natl. Acad. Sci. U. S. A.*
- daCosta, C.J.B., and Baenziger, J.E. (2013). Gating of pentameric ligand-gated ion channels: structural insights and ambiguities. *Struct. Lond. Engl.* *1993* *21*, 1271–1283.
- daCosta, C.J.B., and Sine, S.M. (2013). Stoichiometry for drug potentiation of a pentameric ion channel. *Proc. Natl. Acad. Sci.* *110*, 6595–6600.
- daCosta, C.J.B., Free, C.R., Corradi, J., Bouzat, C., and Sine, S.M. (2011). Single-channel and structural foundations of neuronal $\alpha 7$ acetylcholine receptor potentiation. *J. Neurosci. Off. J. Soc. Neurosci.* *31*, 13870–13879.
- Dawe, G.B., Musgaard, M., Andrews, E.D., Daniels, B.A., Aurousseau, M.R.P., Biggin, P.C., and Bowie, D. (2013). Defining the structural relationship between kainate-receptor deactivation and desensitization. *Nat. Struct. Mol. Biol.* *20*, 1054–1061.
- Dilger, J.P., and Liu, Y. (1992). Desensitization of acetylcholine receptors in BC3H-1 cells. *Pflügers Arch.* *420*, 479–485.
- Dixon, C.L., Harrison, N.L., Lynch, J.W., and Keramidas, A. (2015). Zolpidem and eszopiclone prime $\alpha 1\beta 2\gamma 2$

Desensitization of pentameric ligand-gated ion channels

- GABAA receptors for longer duration of activity. *Br. J. Pharmacol.* *172*, 3522–3536.
- Downing, S.S., Lee, Y.T., Farb, D.H., and Gibbs, T.T. (2005). Benzodiazepine modulation of partial agonist efficacy and spontaneously active GABA(A) receptors supports an allosteric model of modulation. *Br. J. Pharmacol.* *145*, 894–906.
- Du, J., Lü, W., Wu, S., Cheng, Y., and Gouaux, E. (2015). Glycine receptor mechanism elucidated by electron cryo-microscopy. *Nature* *526*, 224–229.
- Duffy, A.M., Fitzgerald, M.L., Chan, J., Robinson, D.C., Milner, T.A., Mackie, K., and Pickel, V.M. (2011). Acetylcholine $\alpha 7$ nicotinic and dopamine D2 receptors are targeted to many of the same postsynaptic dendrites and astrocytes in the rodent prefrontal cortex. *Synap. N. Y. N* *65*, 1350–1367.
- Edelstein, S.J., Schaad, O., Henry, E., Bertrand, D., and Changeux, J.P. (1996). A kinetic mechanism for nicotinic acetylcholine receptors based on multiple allosteric transitions. *Biol. Cybern.* *75*, 361–379.
- Einav, T., and Phillips, R. (2017). Monod-Wyman-Changeux Analysis of Ligand-Gated Ion Channel Mutants. *J. Phys. Chem. B* *121*, 3813–3824.
- Eisenman, L.N., He, Y., Fields, C., Zorumski, C.F., and Mennerick, S. (2003). Activation-Dependent Properties of Pregnenolone Sulfate Inhibition of GABA_A Receptor-Mediated Current. *J. Physiol.* *550*, 679–691.
- Elenes, S., and Auerbach, A. (2002). Desensitization of diliganded mouse muscle nicotinic acetylcholine receptor channels. *J. Physiol.* *541*, 367–383.
- Feltz, A., and Trautmann, A. (1982). Desensitization at the frog neuromuscular junction: a biphasic process. *J. Physiol.* *322*, 257–272.
- Franke, C., Parnas, H., Hovav, G., and Dudel, J. (1993). A molecular scheme for the reaction between acetylcholine and nicotinic channels. *Biophys. J.* *64*, 339–356.
- Galanopoulou, A.S. (2008). GABA(A) receptors in normal development and seizures: friends or foes? *Curr. Neuropharmacol.* *6*, 1–20.
- Gay, E.A., Giniatullin, R., Skorinkin, A., and Yakel, J.L. (2008). Aromatic residues at position 55 of rat $\alpha 7$ nicotinic acetylcholine receptors are critical for maintaining rapid desensitization. *J. Physiol.* *586*, 1105–1115.
- Gielen, M., Le Goff, A., Stroebel, D., Johnson, J.W., Neyton, J., and Paoletti, P. (2008). Structural rearrangements of NR1/NR2A NMDA receptors during allosteric inhibition. *Neuron* *57*, 80–93.
- Gielen, M., Thomas, P., and Smart, T.G. (2015). The desensitization gate of inhibitory Cys-loop receptors. *Nat. Commun.* *6*, 6829.
- Gielen, M.C., Lumb, M.J., and Smart, T.G. (2012). Benzodiazepines Modulate GABAA Receptors by Regulating the Preactivation Step after GABA Binding. *J. Neurosci.* *32*, 5707–5715.
- Gill-Thind, J.K., Dhankher, P., D'Oyley, J.M., Sheppard, T.D., and Millar, N.S. (2015). Structurally similar allosteric modulators of $\alpha 7$ nicotinic acetylcholine receptors exhibit five distinct pharmacological effects. *J. Biol. Chem.* *290*, 3552–3562.
- Giraudat, J., Dennis, M., Heidmann, T., Chang, J.Y., and Changeux, J.P. (1986). Structure of the high-affinity binding site for noncompetitive blockers of the acetylcholine receptor: serine-262 of the delta subunit is labeled by [3H]chlorpromazine. *Proc. Natl. Acad. Sci. U. S. A.* *83*, 2719–2723.
- Glasgow, N.G., Povysheva, N.V., Azofeifa, A.M., and Johnson, J.W. (2017). Memantine and ketamine differentially alter NMDA receptor desensitization. *J. Neurosci.* 1173–17.
- Gonzalez-Gutierrez, G., Wang, Y., Cymes, G.D., Tajkhorshid, E., and Grosman, C. (2017). Chasing the open-state structure of pentameric ligand-gated ion channels. *J. Gen. Physiol.* jgp.201711803.
- Goutman, J.D., and Calvo, D.J. (2004). Studies on the mechanisms of action of picrotoxin, quercetin and pregnanolone at the GABA rho 1 receptor. *Br. J. Pharmacol.* *141*, 717–727.
- Grosman, C., Zhou, M., and Auerbach, A. (2000). Mapping the conformational wave of acetylcholine receptor channel gating. *Nature* *403*, 773–776.
- Hansen, S.B., Wang, H.-L., Taylor, P., and Sine, S.M. (2008). An ion selectivity filter in the extracellular domain of Cys-loop receptors reveals determinants for ion conductance. *J. Biol. Chem.* *283*, 36066–36070.
- Hansen, S.B., Tao, X., and MacKinnon, R. (2011). Structural basis of PIP2 activation of the classical inward rectifier K⁺ channel Kir2.2. *Nature* *477*, 495–498.

Desensitization of pentameric ligand-gated ion channels

- Harpole, T.J., and Grosman, C. (2014). Side-chain conformation at the selectivity filter shapes the permeation free-energy landscape of an ion channel. *Proc. Natl. Acad. Sci. U. S. A.* *111*, E3196-3205.
- Hassaine, G., Deluz, C., Grasso, L., Wyss, R., Tol, M.B., Hovius, R., Graff, A., Stahlberg, H., Tomizaki, T., Desmyter, A., et al. (2014). X-ray structure of the mouse serotonin 5-HT₃ receptor. *Nature* *512*, 276–281.
- Heidmann, T., and Changeux, J.P. (1979). Fast kinetic studies on the interaction of a fluorescent agonist with the membrane-bound acetylcholine receptor from *Torpedo marmorata*. *Eur. J. Biochem.* *94*, 255–279.
- Heidmann, T., and Changeux, J.P. (1980). Interaction of a fluorescent agonist with the membrane-bound acetylcholine receptor from *Torpedo marmorata* in the millisecond time range: resolution of an “intermediate” conformational transition and evidence for positive cooperative effects. *Biochem. Biophys. Res. Commun.* *97*, 889–896.
- Heidmann, T., and Changeux, J.P. (1982). [Molecular model of the regulation of chemical synapse efficiency at the postsynaptic level]. *Comptes Rendus Seances Acad. Sci. Ser. III Sci. Vie* *295*, 665–670.
- Heidmann, T., and Changeux, J.P. (1984). Time-resolved photolabeling by the noncompetitive blocker chlorpromazine of the acetylcholine receptor in its transiently open and closed ion channel conformations. *Proc. Natl. Acad. Sci. U. S. A.* *81*, 1897–1901.
- Heidmann, T., and Changeux, J.P. (1986). Characterization of the transient agonist-triggered state of the acetylcholine receptor rapidly labeled by the noncompetitive blocker [³H]chlorpromazine: additional evidence for the open channel conformation. *Biochemistry (Mosc.)* *25*, 6109–6113.
- Hernandez, C.C., Kong, W., Hu, N., Zhang, Y., Shen, W., Jackson, L., Liu, X., Jiang, Y., and Macdonald, R.L. (2017). Altered Channel Conductance States and Gating of GABAA Receptors by a Pore Mutation Linked to Dravet Syndrome. *ENeuro* *4*.
- Hibbs, R.E., and Gouaux, E. (2011). Principles of activation and permeation in an anion-selective Cys-loop receptor. *Nature* *474*, 54–60.
- Hilf, R.J.C., and Dutzler, R. (2008). X-ray structure of a prokaryotic pentameric ligand-gated ion channel. *Nature* *452*, 375–379.
- Huang, X., Chen, H., Michelsen, K., Schneider, S., and Shaffer, P.L. (2015). Crystal structure of human glycine receptor- $\alpha 3$ bound to antagonist strychnine. *Nature* *526*, 277–280.
- Huang, X., Shaffer, P.L., Ayube, S., Bregman, H., Chen, H., Lehto, S.G., Luther, J.A., Matson, D.J., McDonough, S.I., Michelsen, K., et al. (2017). Crystal structures of human glycine receptor $\alpha 3$ bound to a novel class of analgesic potentiators. *Nat. Struct. Mol. Biol.* *24*, 108–113.
- Huganir, R.L., and Greengard, P. (1990). Regulation of neurotransmitter receptor desensitization by protein phosphorylation. *Neuron* *5*, 555–567.
- Huganir, R.L., Delcour, A.H., Greengard, P., and Hess, G.P. (1986). Phosphorylation of the nicotinic acetylcholine receptor regulates its rate of desensitization. *Nature* *321*, 774–776.
- Hurst, R.S. (2005). A Novel Positive Allosteric Modulator of the 7 Neuronal Nicotinic Acetylcholine Receptor: In Vitro and In Vivo Characterization. *J. Neurosci.* *25*, 4396–4405.
- Imoto, K., Busch, C., Sakmann, B., Mishina, M., Konno, T., Nakai, J., Bujo, H., Mori, Y., Fukuda, K., and Numa, S. (1988). Rings of negatively charged amino acids determine the acetylcholine receptor channel conductance. *Nature* *335*, 645–648.
- Indurthi, D.C., Lewis, T.M., Ahring, P.K., Balle, T., Chebib, M., and Absalom, N.L. (2016). Ligand Binding at the 4-4 Agonist-Binding Site of the 42 nAChR Triggers Receptor Activation through a Pre-Activated Conformational State. *PLoS One* *11*, e0161154.
- Jackson, M.B. (1984). Spontaneous openings of the acetylcholine receptor channel. *Proc. Natl. Acad. Sci. U. S. A.* *81*, 3901–3904.
- Jaiteh, M., Taly, A., and Hémin, J. (2016). Evolution of Pentameric Ligand-Gated Ion Channels: Pro-Loop Receptors. *PLOS ONE* *11*, e0151934.
- Johnson, J.W., and Ascher, P. (1987). Glycine potentiates the NMDA response in cultured mouse brain neurons. *Nature* *325*, 529–531.
- Jones, I.W., and Wonnacott, S. (2004). Precise localization of alpha7 nicotinic acetylcholine receptors on glutamatergic axon terminals in the rat ventral tegmental area. *J. Neurosci. Off. J. Soc. Neurosci.* *24*, 11244–

Desensitization of pentameric ligand-gated ion channels

11252.

Jones, M.V., and Westbrook, G.L. (1995). Desensitized states prolong GABAA channel responses to brief agonist pulses. *Neuron* *15*, 181–191.

Jones, M.V., and Westbrook, G.L. (1996). The impact of receptor desensitization on fast synaptic transmission. *Trends Neurosci.* *19*, 96–101.

Jones, K.A., Wilding, T.J., Huettner, J.E., and Costa, A.M. (1997). Desensitization of kainate receptors by kainate, glutamate and diastereomers of 4-methylglutamate. *Neuropharmacology* *36*, 853–863.

Kalappa, B.I., Sun, F., Johnson, S.R., Jin, K., and Uteshev, V.V. (2013). A positive allosteric modulator of $\alpha 7$ nAChRs augments neuroprotective effects of endogenous nicotinic agonists in cerebral ischaemia: Neuroprotection by PNU-120596 in cerebral ischaemia. *Br. J. Pharmacol.* *169*, 1862–1878.

Karlsson, U., Druzin, M., and Johansson, S. (2011). Cl(-) concentration changes and desensitization of GABA(A) and glycine receptors. *J. Gen. Physiol.* *138*, 609–626.

Katz, B., and Miledi, R. (1973). The binding of acetylcholine to receptors and its removal from the synaptic cleft. *J. Physiol.* *231*, 549–574.

Katz, B., and Thesleff, S. (1957). A study of the desensitization produced by acetylcholine at the motor end-plate. *J. Physiol.* *138*, 63–80.

Kelley, S.P., Dunlop, J.I., Kirkness, E.F., Lambert, J.J., and Peters, J.A. (2003). A cytoplasmic region determines single-channel conductance in 5-HT3 receptors. *Nature* *424*, 321–324.

Kinde, M.N., Chen, Q., Lawless, M.J., Mowrey, D.D., Xu, J., Saxena, S., Xu, Y., and Tang, P. (2015). Conformational Changes Underlying Desensitization of the Pentameric Ligand-Gated Ion Channel ELIC. *Structure* *23*, 995–1004.

King, J.R., and Kabbani, N. (2016). Alpha 7 nicotinic receptor coupling to heterotrimeric G proteins modulates RhoA activation, cytoskeletal motility, and structural growth. *J. Neurochem.* *138*, 532–545.

Kuffler, S.W., and Yoshikami, D. (1975). The number of transmitter molecules in a quantum: an estimate from iontophoretic application of acetylcholine at the neuromuscular synapse. *J. Physiol.* *251*, 465–482.

Kurata, H.T., and Fedida, D. (2006). A structural interpretation of voltage-gated potassium channel inactivation. *Prog. Biophys. Mol. Biol.* *92*, 185–208.

Laha, K.T., Ghosh, B., and Czajkowski, C. (2013). Macroscopic kinetics of pentameric ligand gated ion channels: comparisons between two prokaryotic channels and one eukaryotic channel. *PLoS One* *8*, e80322.

Langlhofer, G., and Villmann, C. (2016). The Intracellular Loop of the Glycine Receptor: It's not all about the Size. *Front. Mol. Neurosci.* *9*, 41.

Lape, R., Colquhoun, D., and Sivilotti, L.G. (2008). On the nature of partial agonism in the nicotinic receptor superfamily. *Nature*.

Lape, R., Krashia, P., Colquhoun, D., and Sivilotti, L.G. (2009). Agonist and blocking actions of choline and tetramethylammonium on human muscle acetylcholine receptors: Activation and block by choline. *J. Physiol.* *587*, 5045–5072.

Laverty, D., Thomas, P., Field, M., Andersen, O.J., Gold, M.G., Biggin, P.C., Gielen, M., and Smart, T.G. (2017). Crystal structures of a GABAA-receptor chimera reveal new endogenous neurosteroid-binding sites. *Nat. Struct. Mol. Biol.*

Leonard, R.J., Labarca, C.G., Charnet, P., Davidson, N., and Lester, H.A. (1988). Evidence that the M2 membrane-spanning region lines the ion channel pore of the nicotinic receptor. *Science* *242*, 1578–1581.

Li, J., Ostmeier, J., Boulanger, E., Rui, H., Perozo, E., and Roux, B. (2017). Chemical substitutions in the selectivity filter of potassium channels do not rule out constricted-like conformations for C-type inactivation. *Proc. Natl. Acad. Sci. U. S. A.*

López-Barneo, J., Hoshi, T., Heinemann, S.H., and Aldrich, R.W. (1993). Effects of external cations and mutations in the pore region on C-type inactivation of Shaker potassium channels. *Receptors Channels* *1*, 61–71.

López-Muñoz, F., Ucha-Udabe, R., and Alamo, C. (2005). The history of barbiturates a century after their clinical introduction. *Neuropsychiatr. Dis. Treat.* *1*, 329–343.

Lynch, J.W., Rajendra, S., Barry, P.H., and Schofield, P.R. (1995). Mutations affecting the glycine receptor

Desensitization of pentameric ligand-gated ion channels

- agonist transduction mechanism convert the competitive antagonist, picrotoxin, into an allosteric potentiator. *J. Biol. Chem.* *270*, 13799–13806.
- Lynch, J.W., Rajendra, S., Pierce, K.D., Handford, C.A., Barry, P.H., and Schofield, P.R. (1997). Identification of intracellular and extracellular domains mediating signal transduction in the inhibitory glycine receptor chloride channel. *EMBO J.* *16*, 110–120.
- Mansoor, S.E., Lü, W., Oosterheert, W., Shekhar, M., Tajkhorshid, E., and Gouaux, E. (2016). X-ray structures define human P2X3 receptor gating cycle and antagonist action. *Nature* *538*, 66–71.
- Martin, N.E., Malik, S., Calimet, N., Changeux, J.-P., and Cecchini, M. (2017). Un-gating and allosteric modulation of a pentameric ligand-gated ion channel captured by molecular dynamics. *PLoS Comput. Biol.* *13*, e1005784.
- Mathers, D., and Barker, J. (1980). (-)Pentobarbital opens ion channels of long duration in cultured mouse spinal neurons. *Science* *209*, 507–509.
- Melyan, Z., Wheal, H.V., and Lancaster, B. (2002). Metabotropic-mediated kainate receptor regulation of IsAHP and excitability in pyramidal cells. *Neuron* *34*, 107–114.
- Menny, A., Lefebvre, S.N., Schmidpeter, P.A., Drège, E., Fourati, Z., Delarue, M., Edelstein, S.J., Nimigeon, C.M., Joseph, D., and Corringer, P.-J. (2017). Identification of a pre-active conformation of a pentameric channel receptor. *ELife* *6*.
- Meyerson, J.R., Kumar, J., Chittori, S., Rao, P., Pierson, J., Bartesaghi, A., Mayer, M.L., and Subramaniam, S. (2014). Structural mechanism of glutamate receptor activation and desensitization. *Nature* *514*, 328–334.
- Meyerson, J.R., Chittori, S., Merk, A., Rao, P., Han, T.H., Serpe, M., Mayer, M.L., and Subramaniam, S. (2016). Structural basis of kainate subtype glutamate receptor desensitization. *Nature* *537*, 567–571.
- Middleton, R.E., Strnad, N.P., and Cohen, J.B. (1999). Photoaffinity labeling the torpedo nicotinic acetylcholine receptor with [(3)H]tetracaine, a nondesensitizing noncompetitive antagonist. *Mol. Pharmacol.* *56*, 290–299.
- Miller, P.S., and Aricescu, A.R. (2014). Crystal structure of a human GABAA receptor. *Nature* *512*, 270–275.
- Miller, P.S., Scott, S., Masiulis, S., De Colibus, L., Pardon, E., Steyaert, J., and Aricescu, A.R. (2017). Structural basis for GABAA receptor potentiation by neurosteroids. *Nat. Struct. Mol. Biol.*
- Miyazawa, A., Fujiyoshi, Y., and Unwin, N. (2003). Structure and gating mechanism of the acetylcholine receptor pore. *Nature* *423*, 949–955.
- Monod, J., Wyman, J., and Changeux, J.P. (1965). ON THE NATURE OF ALLOSTERIC TRANSITIONS: A PLAUSIBLE MODEL. *J. Mol. Biol.* *12*, 88–118.
- Morales-Perez, C.L., Noviello, C.M., and Hibbs, R.E. (2016). X-ray structure of the human $\alpha 4\beta 2$ nicotinic receptor. *Nature* *538*, 411–415.
- Mortensen, M., Kristiansen, U., Ebert, B., Frølund, B., Krogsgaard-Larsen, P., and Smart, T.G. (2004). Activation of single heteromeric GABA(A) receptor ion channels by full and partial agonists. *J. Physiol.* *557*, 389–413.
- Mortensen, M., Patel, B., and Smart, T.G. (2011). GABA Potency at GABA(A) Receptors Found in Synaptic and Extrasynaptic Zones. *Front. Cell. Neurosci.* *6*, 1.
- Moss, S.J., Smart, T.G., Blackstone, C.D., and Haganir, R.L. (1992). Functional modulation of GABAA receptors by cAMP-dependent protein phosphorylation. *Science* *257*, 661–665.
- Mukhtasimova, N., Lee, W.Y., Wang, H.-L., and Sine, S.M. (2009). Detection and trapping of intermediate states priming nicotinic receptor channel opening. *Nature* *459*, 451–454.
- Nayak, T.K., and Auerbach, A. (2017). Cyclic activation of endplate acetylcholine receptors. *Proc. Natl. Acad. Sci.* *201711228*.
- Nemecz, Á., Prevost, M.S., Menny, A., and Corringer, P.-J. (2016). Emerging Molecular Mechanisms of Signal Transduction in Pentameric Ligand-Gated Ion Channels. *Neuron* *90*, 452–470.
- Newcombe, J., Chatzidaki, A., Sheppard, T.D., Topf, M., and Millar, N.S. (2017). Diversity of nicotinic acetylcholine receptor positive allosteric modulators revealed by mutagenesis and a revised structural model. *Mol. Pharmacol.* *mol.117.110551*.
- Nicolai, C., and Sachs, F. (2013). SOLVING ION CHANNEL KINETICS WITH THE QuB SOFTWARE.

Desensitization of pentameric ligand-gated ion channels

Biophys. Rev. Lett. *08*, 191–211.

Nuss, P. (2015). Anxiety disorders and GABA neurotransmission: a disturbance of modulation. *Neuropsychiatr. Dis. Treat.* *11*, 165–175.

Opekarová, M., and Tanner, W. (2003). Specific lipid requirements of membrane proteins—a putative bottleneck in heterologous expression. *Biochim. Biophys. Acta BBA - Biomembr.* *1610*, 11–22.

Othman, N.A., Gallacher, M., Deeb, T.Z., Baptista-Hon, D.T., Perry, D.C., and Hales, T.G. (2012). Influences on blockade by *t*-butylbicyclo-phosphoro-thionate of GABA_A receptor spontaneous gating, agonist activation and desensitization: GABA_A receptor blockade. *J. Physiol.* *590*, 163–178.

Papke, D., and Grosman, C. (2014). The role of intracellular linkers in gating and desensitization of human pentameric ligand-gated ion channels. *J. Neurosci. Off. J. Soc. Neurosci.* *34*, 7238–7252.

Papke, D., Gonzalez-Gutierrez, G., and Grosman, C. (2011). Desensitization of neurotransmitter-gated ion channels during high-frequency stimulation: a comparative study of Cys-loop, AMPA and purinergic receptors. *J. Physiol.* *589*, 1571–1585.

Parker, I., Gunderson, C.B., and Miledi, R. (1986). Actions of pentobarbital on rat brain receptors expressed in *Xenopus* oocytes. *J. Neurosci. Off. J. Soc. Neurosci.* *6*, 2290–2297.

Pau, V., Zhou, Y., Ramu, Y., Xu, Y., and Lu, Z. (2017). Crystal structure of an inactivated mutant mammalian voltage-gated K⁺ channel. *Nat. Struct. Mol. Biol.*

Payandeh, J., Gamal El-Din, T.M., Scheuer, T., Zheng, N., and Catterall, W.A. (2012). Crystal structure of a voltage-gated sodium channel in two potentially inactivated states. *Nature* *486*, 135–139.

Plested, A.J.R. (2014). Don't flip out: AChRs are primed to catch and hold your attention. *Biophys. J.* *107*, 8–9.

Plested, A.J.R. (2016). Structural mechanisms of activation and desensitization in neurotransmitter-gated ion channels. *Nat. Struct. Mol. Biol.* *23*, 494–502.

Posson, D.J., McCoy, J.G., and Nimigeon, C.M. (2013). The voltage-dependent gate in MthK potassium channels is located at the selectivity filter. *Nat. Struct. Mol. Biol.* *20*, 159–166.

Prevost, M.S., Sauguet, L., Nury, H., Van Renterghem, C., Huon, C., Poitevin, F., Baaden, M., Delarue, M., and Corringer, P.-J. (2012). A locally closed conformation of a bacterial pentameric proton-gated ion channel. *Nat. Struct. Mol. Biol.* *19*, 642–649.

Prince, R.J., and Sine, S.M. (1999). Acetylcholine and epibatidine binding to muscle acetylcholine receptors distinguish between concerted and uncoupled models. *J. Biol. Chem.* *274*, 19623–19629.

Purohit, P., and Auerbach, A. (2009). Unliganded gating of acetylcholine receptor channels. *Proc. Natl. Acad. Sci.* *106*, 115–120.

Purohit, Y., and Grosman, C. (2006). Block of muscle nicotinic receptors by choline suggests that the activation and desensitization gates act as distinct molecular entities. *J. Gen. Physiol.* *127*, 703–717.

Purohit, P., Bruhova, I., Gupta, S., and Auerbach, A. (2014). Catch-and-hold activation of muscle acetylcholine receptors having transmitter binding site mutations. *Biophys. J.* *107*, 88–99.

Qian, H. (2004). Picrotoxin Accelerates Relaxation of GABAC Receptors. *Mol. Pharmacol.* *67*, 470–479.

Rayes, D., De Rosa, M.J., Sine, S.M., and Bouzat, C. (2009). Number and locations of agonist binding sites required to activate homomeric Cys-loop receptors. *J. Neurosci. Off. J. Soc. Neurosci.* *29*, 6022–6032.

Revah, F., Galzi, J.L., Giraudat, J., Haumont, P.Y., Lederer, F., and Changeux, J.P. (1990). The noncompetitive blocker [3H]chlorpromazine labels three amino acids of the acetylcholine receptor gamma subunit: implications for the alpha-helical organization of regions MII and for the structure of the ion channel. *Proc. Natl. Acad. Sci. U. S. A.* *87*, 4675–4679.

Revah, F., Bertrand, D., Galzi, J.L., Devillers-Thiéry, A., Mulle, C., Hussy, N., Bertrand, S., Ballivet, M., and Changeux, J.P. (1991). Mutations in the channel domain alter desensitization of a neuronal nicotinic receptor. *Nature* *353*, 846–849.

Rho, J.M., Donevan, S.D., and Rogawski, M.A. (1996). Direct activation of GABA_A receptors by barbiturates in cultured rat hippocampal neurons. *J. Physiol.* *497*, 509–522.

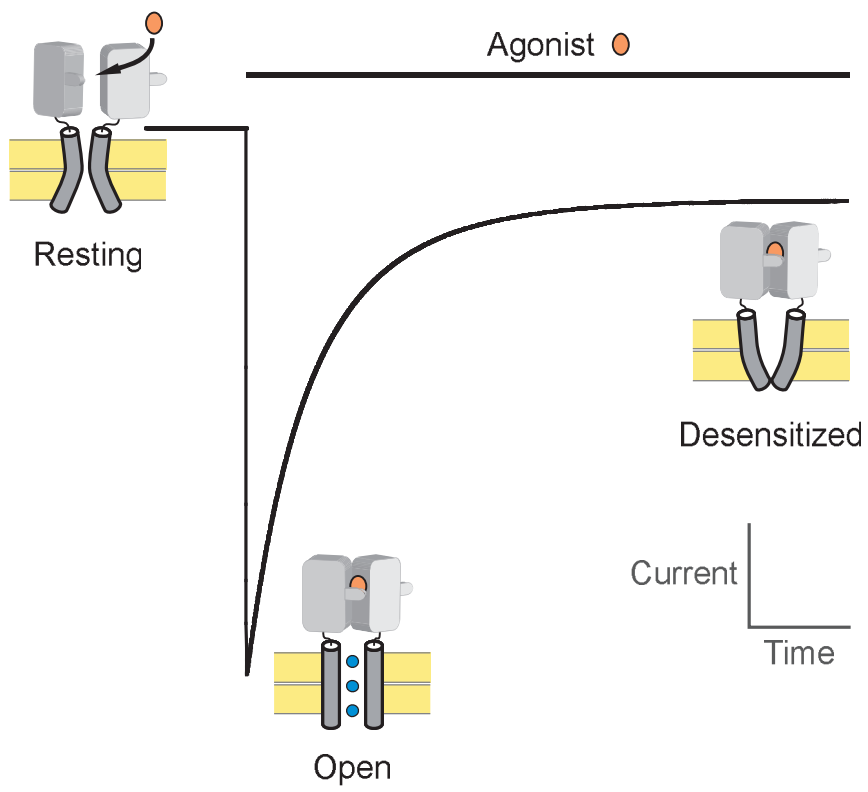
Rodríguez-Moreno, A., and Lerma, J. (1998). Kainate receptor modulation of GABA release involves a metabotropic function. *Neuron* *20*, 1211–1218.

Desensitization of pentameric ligand-gated ion channels

- Rossokhin, A.V., and Zhorov, B.S. (2016). Side chain flexibility and the pore dimensions in the GABAA receptor. *J. Comput. Aided Mol. Des.* 30, 559–567.
- Sather, W., Dieudonné, S., MacDonald, J.F., and Ascher, P. (1992). Activation and desensitization of N-methyl-D-aspartate receptors in nucleated outside-out patches from mouse neurones. *J. Physiol.* 450, 643–672.
- Sauguet, L., Poitevin, F., Murail, S., Van Renterghem, C., Moraga-Cid, G., Malherbe, L., Thompson, A.W., Koehl, P., Corringer, P.-J., Baaden, M., et al. (2013). Structural basis for ion permeation mechanism in pentameric ligand-gated ion channels. *EMBO J.* 32, 728–741.
- Sauguet, L., Shahsavar, A., Poitevin, F., Huon, C., Menny, A., Nemezc, À., Haouz, A., Changeux, J.-P., Corringer, P.-J., and Delarue, M. (2014). Crystal structures of a pentameric ligand-gated ion channel provide a mechanism for activation. *Proc. Natl. Acad. Sci. U. S. A.* 111, 966–971.
- Saul, B., Kuner, T., Sobetzko, D., Brune, W., Hanefeld, F., Meinck, H.M., and Becker, C.M. (1999). Novel GLRA1 missense mutation (P250T) in dominant hyperekplexia defines an intracellular determinant of glycine receptor channel gating. *J. Neurosci. Off. J. Soc. Neurosci.* 19, 869–877.
- Shen, W., Mennerick, S., Covey, D.F., and Zorumski, C.F. (2000). Pregnenolone sulfate modulates inhibitory synaptic transmission by enhancing GABA(A) receptor desensitization. *J. Neurosci. Off. J. Soc. Neurosci.* 20, 3571–3579.
- Shytle, R.D., Mori, T., Townsend, K., Vendrame, M., Sun, N., Zeng, J., Ehrhart, J., Silver, A.A., Sanberg, P.R., and Tan, J. (2004). Cholinergic modulation of microglial activation by alpha 7 nicotinic receptors. *J. Neurochem.* 89, 337–343.
- Smart, T.G., and Constanti, A. (1986). Studies on the mechanism of action of picrotoxinin and other convulsants at the crustacean muscle GABA receptor. *Proc. R. Soc. Lond. B Biol. Sci.* 227, 191–216.
- Smart, T.G., and Paoletti, P. (2012). Synaptic neurotransmitter-gated receptors. *Cold Spring Harb. Perspect. Biol.* 4.
- Sun, Y., Olson, R., Horning, M., Armstrong, N., Mayer, M., and Gouaux, E. (2002). Mechanism of glutamate receptor desensitization. *Nature* 417, 245–253.
- Taly, A., Corringer, P.-J., Grutter, T., de Carvalho, L.P., Karplus, M., and Changeux, J.-P. (2006). Implications of the quaternary twist allosteric model for the physiology and pathology of nicotinic acetylcholine receptors. *Proc. Natl. Acad. Sci.* 103, 16965–16970.
- Taly, A., Corringer, P.-J., Guedin, D., Lestage, P., and Changeux, J.-P. (2009). Nicotinic receptors: allosteric transitions and therapeutic targets in the nervous system. *Nat. Rev. Drug Discov.* 8, 733–750.
- Tasneem, A., Iyer, L.M., Jakobsson, E., and Aravind, L. (2005). Identification of the prokaryotic ligand-gated ion channels and their implications for the mechanisms and origins of animal Cys-loop ion channels. *Genome Biol.* 6, R4.
- Tong, G., and Jahr, C.E. (1994). Regulation of glycine-insensitive desensitization of the NMDA receptor in outside-out patches. *J. Neurophysiol.* 72, 754–761.
- Tong, G., Shepherd, D., and Jahr, C.E. (1995). Synaptic desensitization of NMDA receptors by calcineurin. *Science* 267, 1510–1512.
- Toth, B., and Csányi, L. (2012). Pore collapse underlies irreversible inactivation of TRPM2 cation channel currents. *Proc. Natl. Acad. Sci.* 109, 13440–13445.
- Trick, J.L., Chelvanithilan, S., Klesse, G., Aryal, P., Wallace, E.J., Tucker, S.J., and Sansom, M.S.P. (2016). Functional Annotation of Ion Channel Structures by Molecular Simulation. *Struct. Lond. Engl.* 24, 2207–2216.
- Trueta, C., and De-Miguel, F.F. (2012). Extrasynaptic exocytosis and its mechanisms: a source of molecules mediating volume transmission in the nervous system. *Front. Physiol.* 3, 319.
- Twomey, E.C., Yelshanskaya, M.V., Grassucci, R.A., Frank, J., and Sobolevsky, A.I. (2017). Channel opening and gating mechanism in AMPA-subtype glutamate receptors. *Nature* 549, 60–65.
- Twyman, R.E., and Macdonald, R.L. (1992). Neurosteroid regulation of GABAA receptor single-channel kinetic properties of mouse spinal cord neurons in culture. *J. Physiol.* 456, 215–245.
- Vizi, E.S., Fekete, A., Karoly, R., and Mike, A. (2010). Non-synaptic receptors and transporters involved in brain functions and targets of drug treatment. *Br. J. Pharmacol.* 160, 785–809.

Desensitization of pentameric ligand-gated ion channels

- Wang, Q., and Lynch, J.W. (2011). Activation and desensitization induce distinct conformational changes at the extracellular-transmembrane domain interface of the glycine receptor. *J. Biol. Chem.* *286*, 38814–38824.
- Wang, D.-S., Mangin, J.-M., Moonen, G., Rigo, J.-M., and Legendre, P. (2006). Mechanisms for picrotoxin block of alpha2 homomeric glycine receptors. *J. Biol. Chem.* *281*, 3841–3855.
- Wang, D.-S., Buckinx, R., Lecorronc, H., Mangin, J.-M., Rigo, J.-M., and Legendre, P. (2007). Mechanisms for picrotoxin and picrotin blocks of alpha2 homomeric glycine receptors. *J. Biol. Chem.* *282*, 16016–16035.
- Xia, P., Chen, H. -s. V., Zhang, D., and Lipton, S.A. (2010). Memantine Preferentially Blocks Extrasynaptic over Synaptic NMDA Receptor Currents in Hippocampal Autapses. *J. Neurosci.* *30*, 11246–11250.
- Xu, X.-J., Roberts, D., Zhu, G.-N., and Chang, Y.-C. (2016). Competitive antagonists facilitate the recovery from desensitization of $\alpha 1\beta 2\gamma 2$ GABAA receptors expressed in *Xenopus* oocytes. *Acta Pharmacol. Sin.* *37*, 1020–1030.
- Yakel, J.L., Lagrutta, A., Adelman, J.P., and North, R.A. (1993). Single amino acid substitution affects desensitization of the 5-hydroxytryptamine type 3 receptor expressed in *Xenopus* oocytes. *Proc. Natl. Acad. Sci. U. S. A.* *90*, 5030–5033.
- Yamodo, I.H., Chiara, D.C., Cohen, J.B., and Miller, K.W. (2010). Conformational Changes in the Nicotinic Acetylcholine Receptor during Gating and Desensitization. *Biochemistry (Mosc.)* *49*, 156–165.
- Yao, J., and Qin, F. (2009). Interaction with phosphoinositides confers adaptation onto the TRPV1 pain receptor. *PLoS Biol.* *7*, e46.
- Young, G.T., Zwart, R., Walker, A.S., Sher, E., and Millar, N.S. (2008). Potentiation of alpha7 nicotinic acetylcholine receptors via an allosteric transmembrane site. *Proc. Natl. Acad. Sci. U. S. A.* *105*, 14686–14691.
- Zhang, J., Xue, F., Whiteaker, P., Li, C., Wu, W., Shen, B., Huang, Y., Lukas, R.J., and Chang, Y. (2011). Desensitization of alpha7 nicotinic receptor is governed by coupling strength relative to gate tightness. *J. Biol. Chem.* *286*, 25331–25340.
- Zhang, J., Xue, F., Liu, Y., Yang, H., and Wang, X. (2013). The Structural Mechanism of the Cys-Loop Receptor Desensitization. *Mol. Neurobiol.* *48*, 97–108.
- Zhang, X., Ren, W., DeCaen, P., Yan, C., Tao, X., Tang, L., Wang, J., Hasegawa, K., Kumasaka, T., He, J., et al. (2012). Crystal structure of an orthologue of the NaChBac voltage-gated sodium channel. *Nature* *486*, 130–134.
- Zhu, W.J., and Vicini, S. (1997). Neurosteroid prolongs GABAA channel deactivation by altering kinetics of desensitized states. *J. Neurosci. Off. J. Soc. Neurosci.* *17*, 4022–4031.
- Zhu, S., Stein, R.A., Yoshioka, C., Lee, C.-H., Goehring, A., Mchaourab, H.S., and Gouaux, E. (2016). Mechanism of NMDA Receptor Inhibition and Activation. *Cell* *165*, 704–714.



Abstract Figure

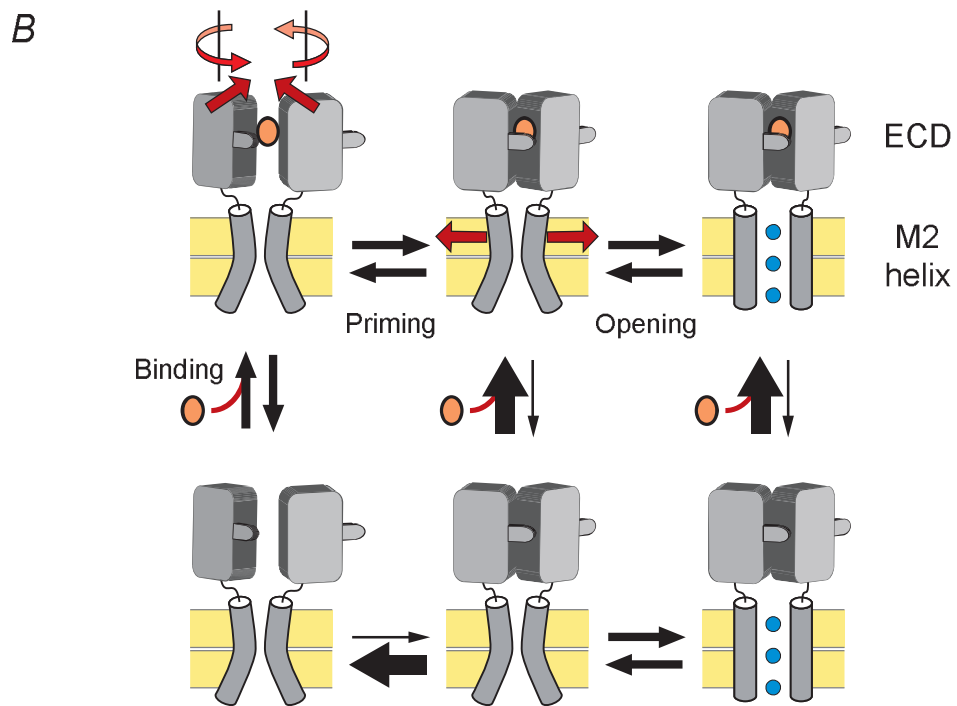
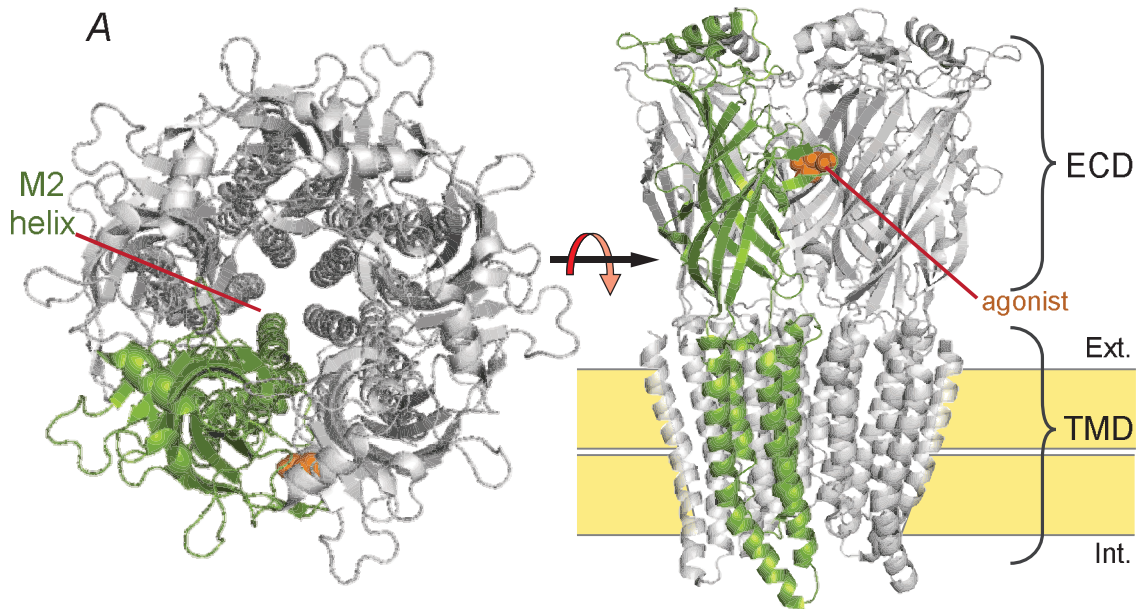


Figure 1

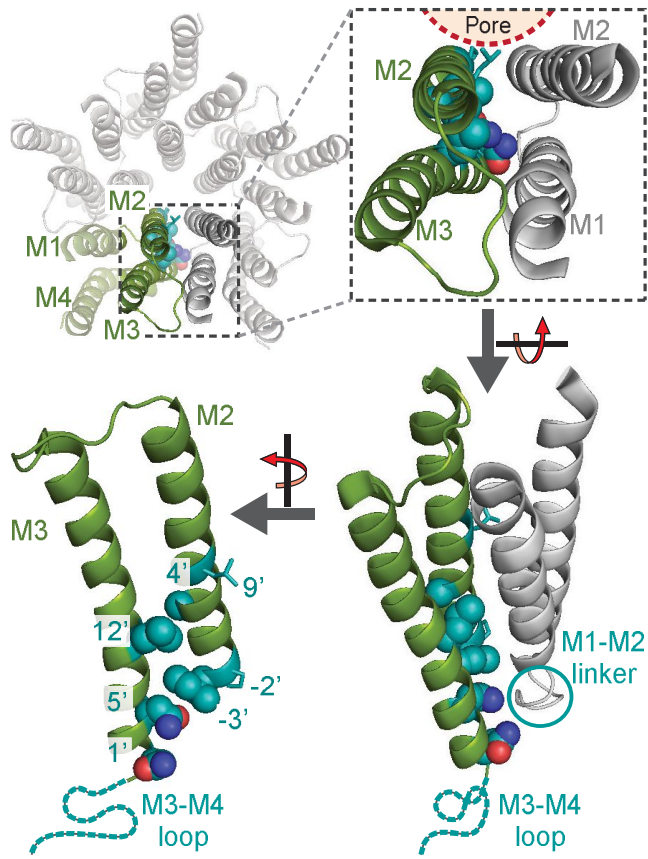


Figure 2

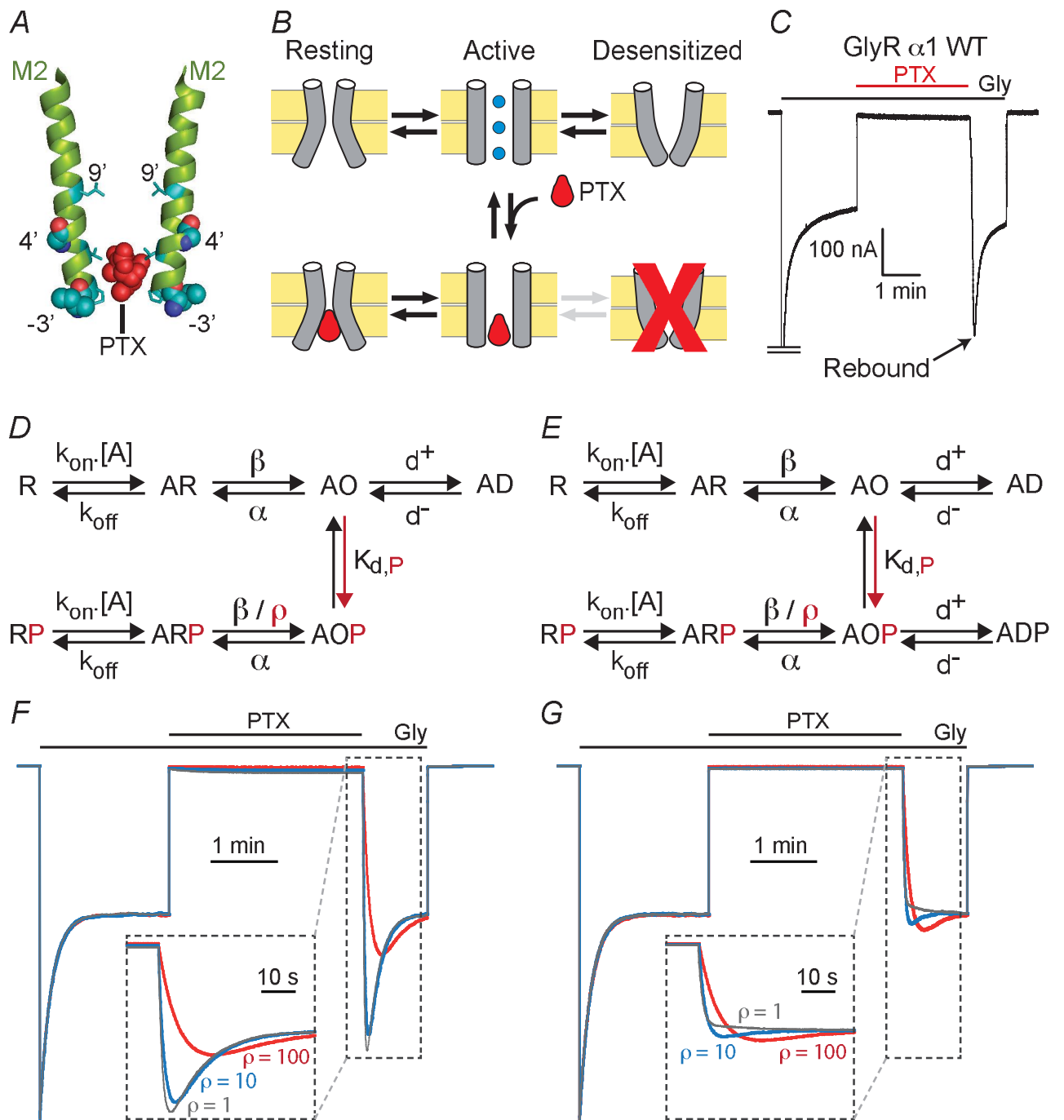


Figure 3

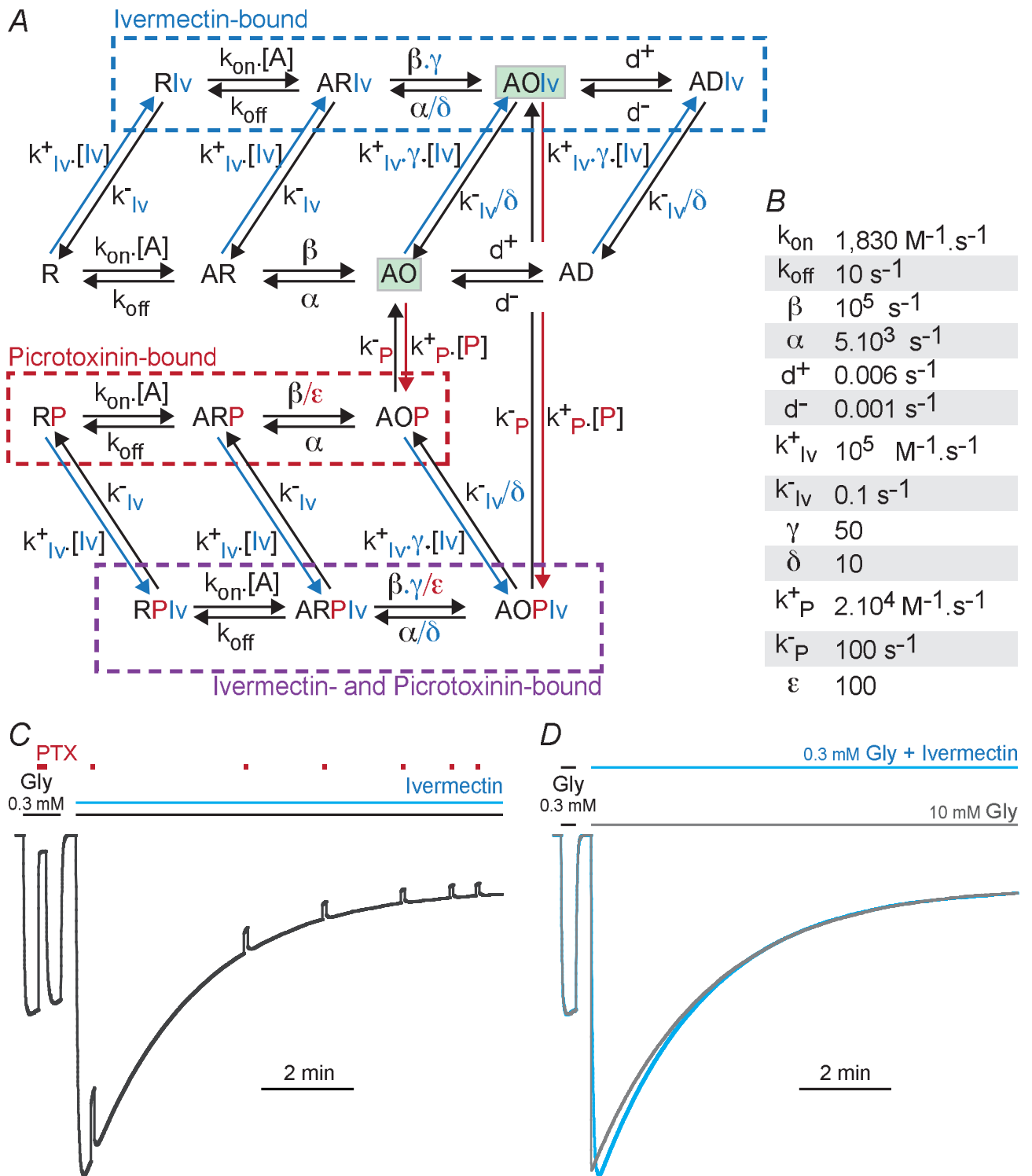


Figure 4

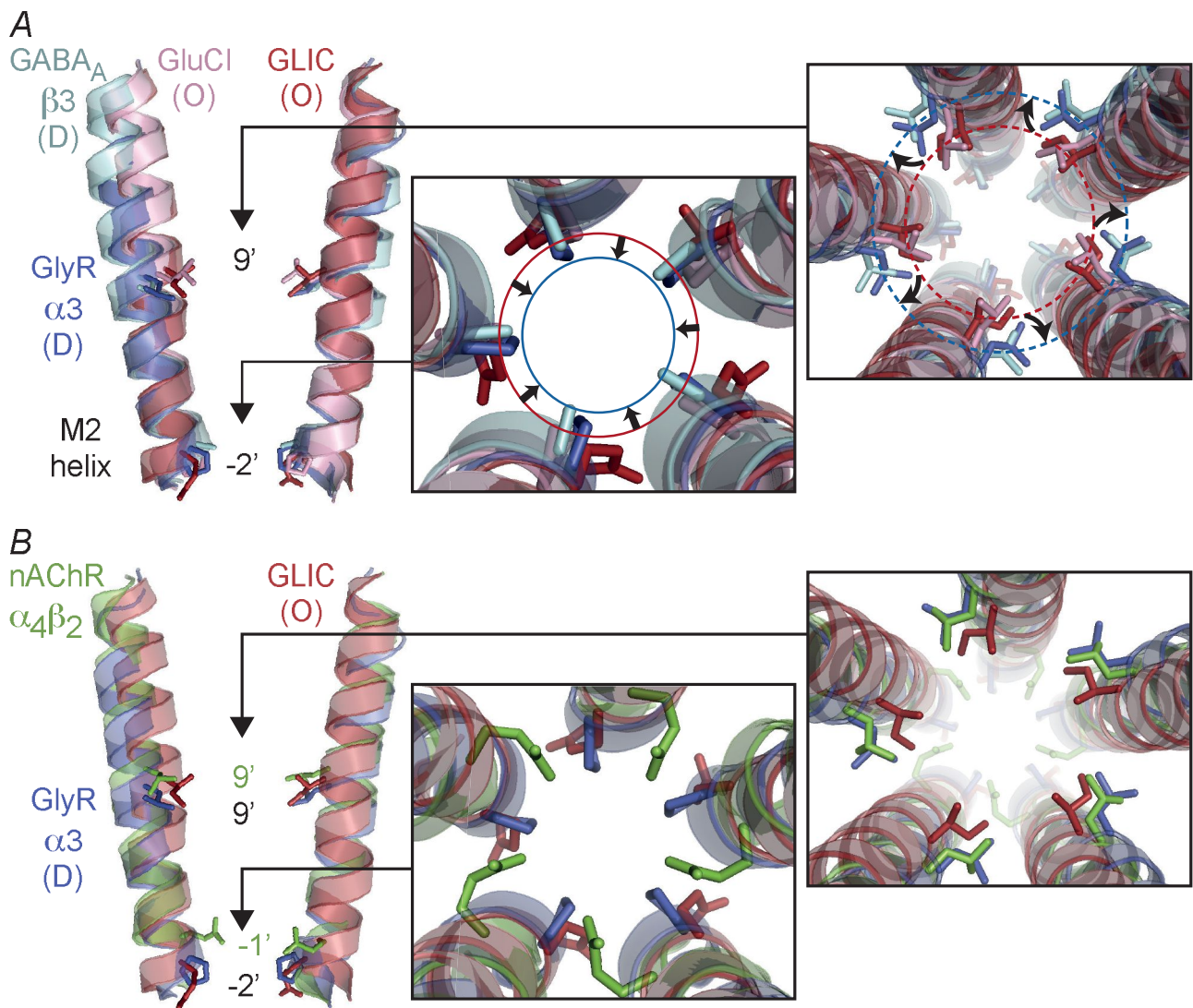


Figure 5

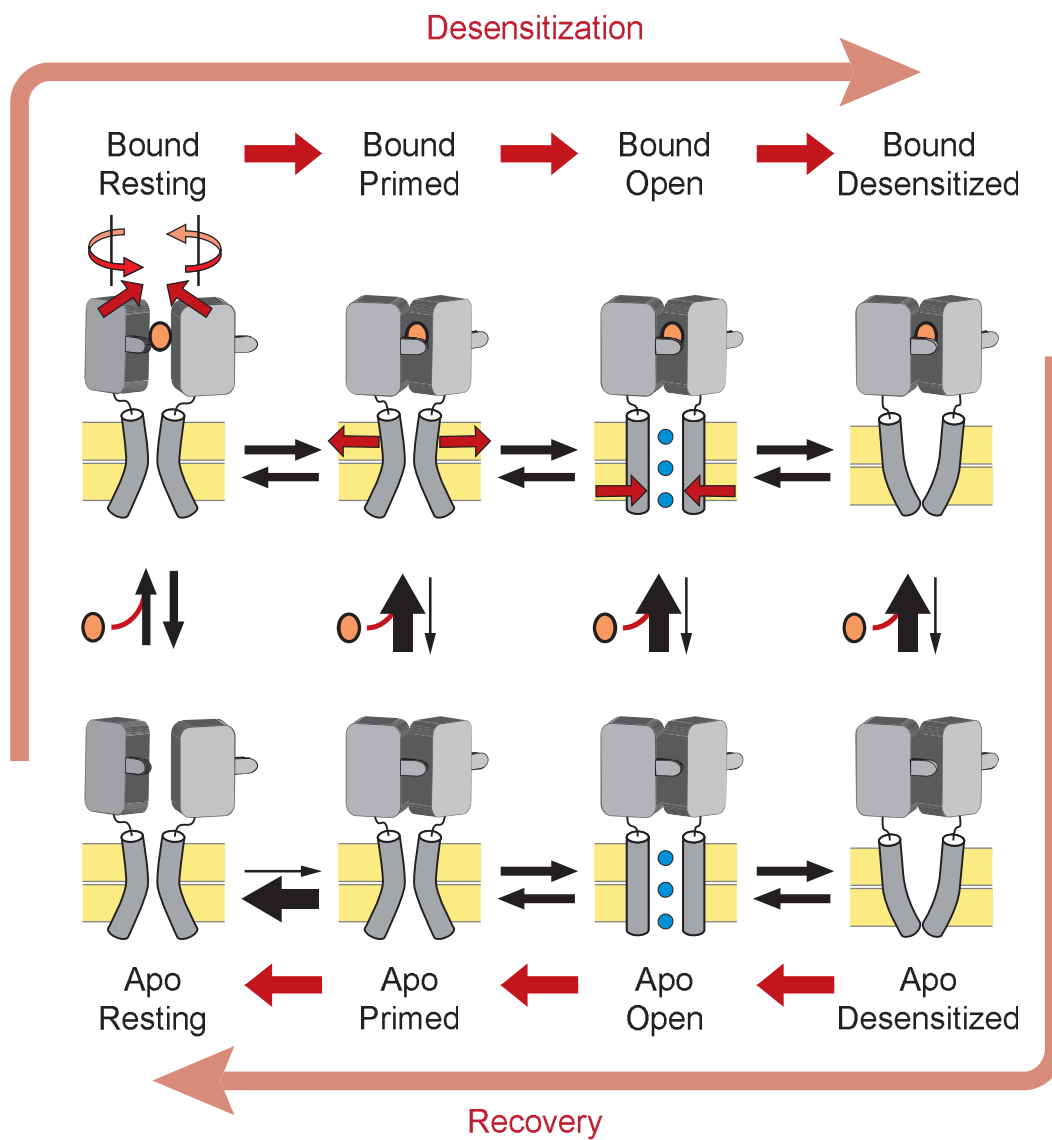
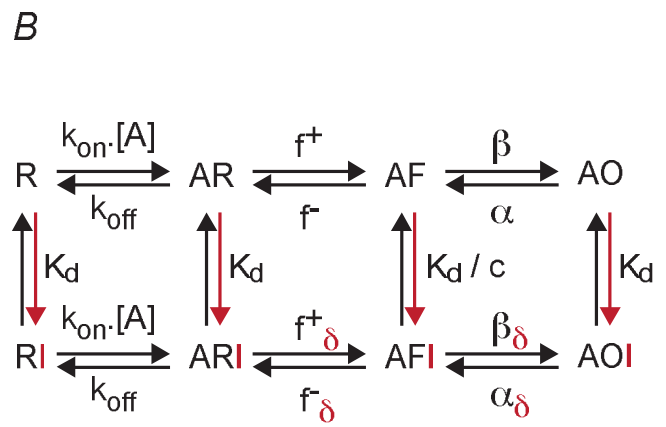
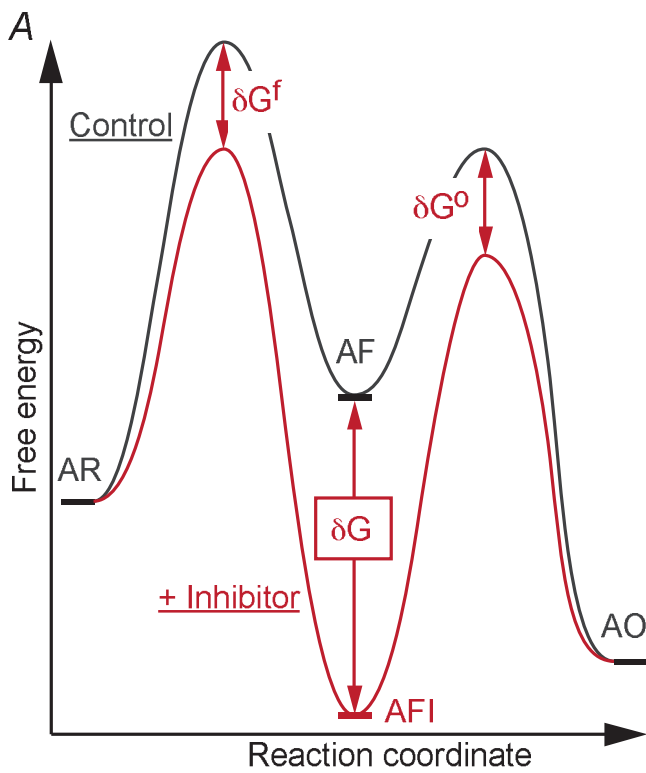


Figure 6



$$\begin{aligned}
 f_{\delta}^+ &= f^+ \cdot \exp(\delta G^f / RT) \\
 f_{\delta}^- &= f^- \cdot \exp(-\delta G / RT) \cdot \exp(\delta G^f / RT)
 \end{aligned}$$

$$\begin{aligned}
 \beta_{\delta} &= \beta \cdot \exp(-\delta G / RT) \cdot \exp(\delta G^0 / RT) \\
 \alpha_{\delta} &= \alpha \cdot \exp(\delta G^0 / RT)
 \end{aligned}$$

C

$$c = \exp(\delta G / RT) > 1$$

$$F = \frac{f^+}{f^-} \text{ and } F_{\delta} = \frac{f_{\delta}^+}{f_{\delta}^-} \rightarrow F_{\delta} = c \cdot F$$

$$E = \frac{\beta}{\alpha} \text{ and } E_{\delta} = \frac{\beta_{\delta}}{\alpha_{\delta}} \rightarrow E_{\delta} = E / c$$

D

In control: $[I] = 0$

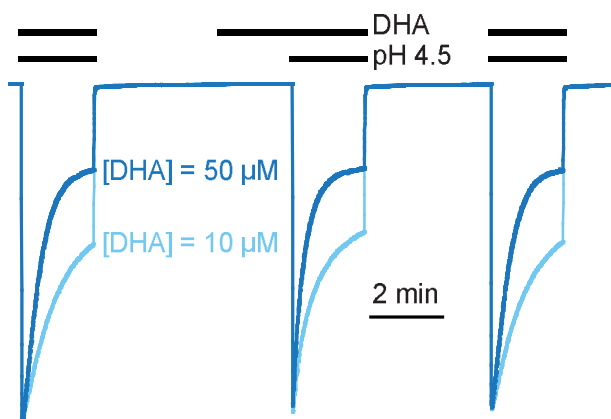
High inhibition: $[I] = \infty$

$$P_{o,\max}^{\text{ctrl}} = \frac{E \cdot F}{1 + F + E \cdot F} > P_{o,\max}^I = \frac{E \cdot F}{1 + c \cdot F + E \cdot F}$$

$$EC_{50,A}^{\text{ctrl}} = \frac{k_{\text{off}} / k_{\text{on}}}{1 + F + E \cdot F} > EC_{50,A}^I = \frac{k_{\text{off}} / k_{\text{on}}}{1 + c \cdot F + E \cdot F}$$

Figure 7

A DHA stabilizes the desensitized state



B DHA stabilizes the preactive state

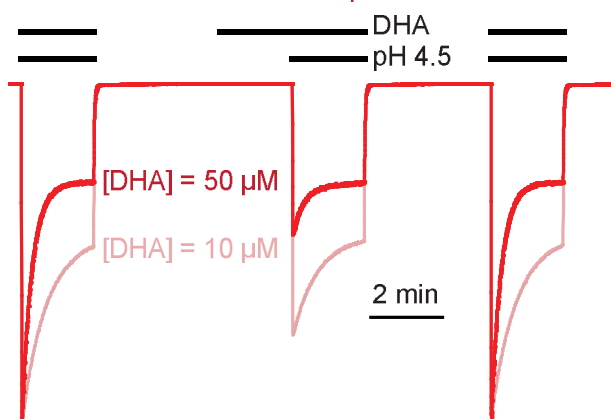


Figure 10

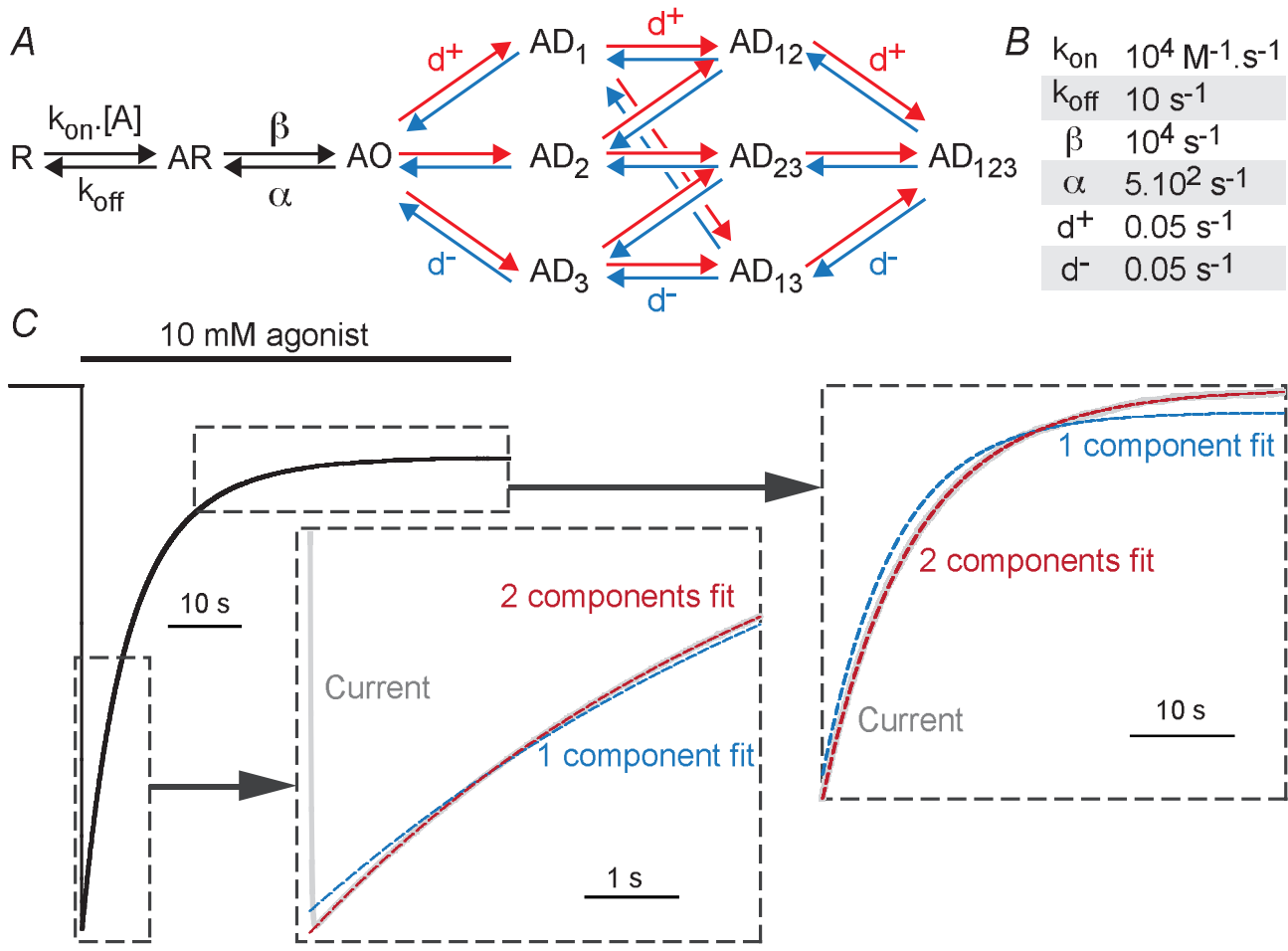
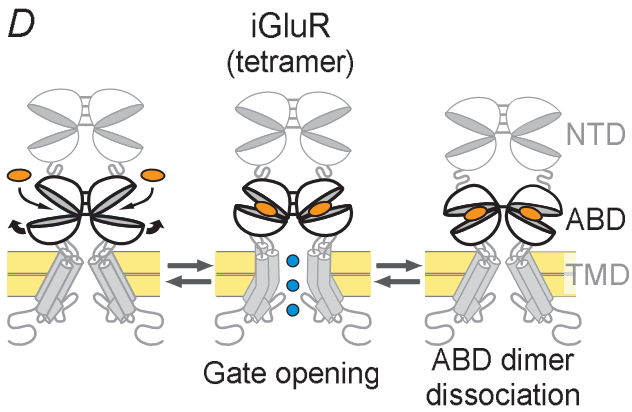
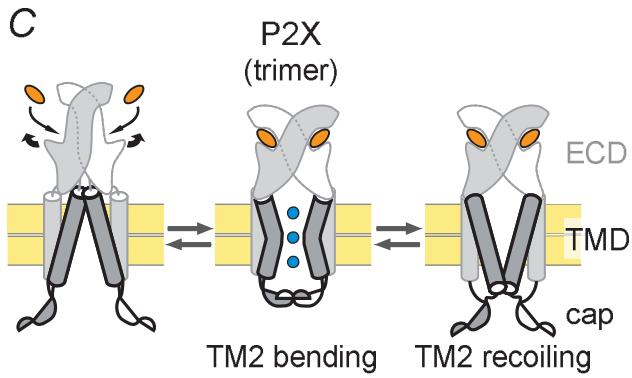
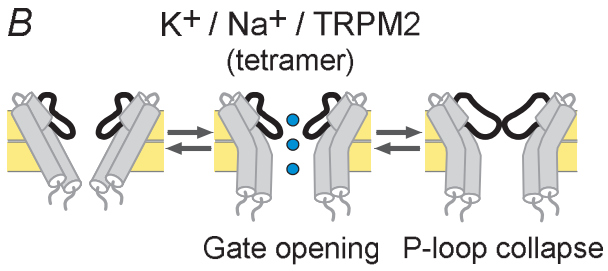
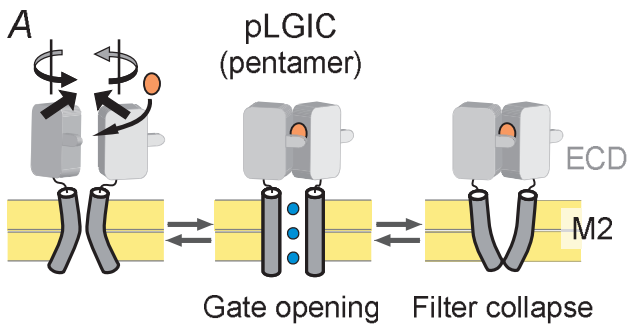


Figure 11



Resting \rightleftharpoons Open \rightleftharpoons Desensitized / Inactivated

Figure 12